2017

Processing, microstructure and mechanical properties of beta-type titanium porous structures made by additive manufacturing

Yujing Liu
Edith Cowan University

PROCESSING, MICROSTRUCTURE AND MECHANICAL PROPERTIES OF BETA-TYPE TITANIUM POROUS STRUCTURES MADE BY ADDITIVE MANUFACTURING

By

Yujing Liu

A thesis submitted to the Edith Cowan University in
fulfilment of the requirements for the degree doctor of philosophy
Edith Cowan University (ECU)
(School of Engineering)

Principal supervisor:
Associate Professor Lai-Chang Zhang
Edith Cowan University, Australia

Associate supervisor:
Professor Yu-Lin Hao
Institute of Metal Research Chinese Academy of Sciences

January, 2017

Abstract

Tissue engineering through the application of a low modulus, high strength format as a potential approach for increasing the durability of bone implants has been attracting significant attention. Titanium alloys are widely used for biomedical applications because of their low modulus, high biocompatibility, specific strength and corrosion resistance. These reasons affirm why titanium alloy is selected as the specific material to research. The development of low modulus biomaterials is considered to be an effective method to remove the mismatch between biomaterial implants and surrounding bone tissue, thereby reducing the risk of bone resorption. So far, Ti–24Nb–4Zr–8Sn alloy (abbreviated here after as Ti2448) is considered to be a biomedical titanium alloy with low modulus, and was invented for biomaterial application. However, the modulus of Ti2448 (42-50 GPa) is still higher than that of bone (1-30 GPa). A scaffold is an ideal structure for bone implants; such a structure can further reduce the modulus of an implant. This structure also has the desired effect of promoting bone in-growth. Additive manufacturing could prepare porous titanium parts with mechanical properties close to those of bone tissue. However, the properties of scaffolds are affected by manufacturing strategies and parameters such as the scanning speed, the input power, the layer thickness, the scanning strategy, the temperature of the platform and the hatch distance. Each of these parameters can affect a scaffold's properties and performance in terms of density, hardness, super-elastic property, compressive and fatigue properties. For the Ti2448 alloy, all of these manufacturing parameters are still not clear enough to develop the perfect porous structure. This study will examine the performance of biomaterial Ti2448 scaffolds by tuning the main parameters of additive manufacturing (AM) systems through an analysis of the microstructure and the mechanical properties of the produced components.

Declaration

I certify that this PhD thesis does not, to the best of my knowledge and belief:

i. Incorporate without acknowledgment any material previously submitted for a degree or diploma in any institution of higher education;

ii. Contain any material previously published or written by another person except where due reference is made in the text of this thesis;

iii. Contain any defamatory material.

Yujing Liu

08/03/2017

[redacted]

List of abbreviations

Abbreviations

AM	Additive manufacturing
bcc	Body centred cubic crystal
CAD	Computer aided design
CP-Ti	Commercially pure titanium
EBM	Electron beam melting
HAZ	Heat affected zone
hcp	Hexagonal closed packed crystal
HIP	Hot isostatic pressing
Hv	Vickers hardness scale
OM	Optical microscopy
Micro-CT	Micro computed tomography
PRS	Powder removing system
RM	Rapid Manufacturing
SEM	Scanning electron microscopy
SLM	Selective laser melting
TEM	Transmission electron microscopy
XRD	X-ray diffraction

Table of Content

List of Figures

List of Tables

List of Publications

[1] **Y.J. Liu**, H.L. Wang, S.J. Li, S.G. Wang, W.J. Wang, W.T. Hou, Y.L. Hao, R. Yang, L.C. Zhang, Compressive and fatigue behavior of beta-type titanium porous structures fabricated by electron beam melting, Acta Materialia.126 (2017) 58-66.

[2] **Y.J. Liu**, S.J. Li, H.L. Wang, W.T. Hou, Y.L. Hao, R. Yang, T.B. Sercombe, L.C. Zhang, Microstructure, defects and mechanical behavior of beta-type titanium porous structures manufactured by electron beam melting and selective laser melting, Acta Materialia. 113 (2016) 56-67.

[3] **Y.J. Liu**, X.P. Li, L.C. Zhang, T.B. Sercombe, Processing and properties of topologically optimised biomedical Ti–24Nb–4Zr–8Sn scaffolds manufactured by selective laser melting, Materials Science and Engineering: A. 642 (2015) 268-278.

[4] **Y.J. Liu**, S.J. Li, W.T. Hou, S.G. Wang, Y.L. Hao, R. Yang, T. Sercombe, L.C. Zhang, Electron beam melted beta-type Ti-24Nb-4Zr-8Sn porous structures with high strength-to-modulus ratio, Journal of Materials Science and Technology. 32 (2016) 505-508

[5] **Y.J. Liu**, W. Wang, L.C. Zhang, Additive manufacturing techniques and their biomedical applications, Family Medicine and Community Health, In press (2016).

[6] X. Li, X. Wang, M. Saunders, A. Suvorova, L. Zhang, **Y.J. Liu**, M. Fang, Z. Huang, T.B. Sercombe, A selective laser melting and solution heat treatment refined Al–12Si alloy with a controllable ultrafine eutectic microstructure and 25% tensile ductility, Acta Materialia. 95 (2015) 74-82.

[7] S. Ehtemam-Haghighi, **Y.J. Liu**, G. Cao, L.-C. Zhang, Influence of Nb on the $\beta \rightarrow \alpha''$

martensitic phase transformation and properties of the newly designed Ti-Fe-Nb alloys, Materials Science and Engineering: C. 60 (2015) 503-510.

[8] S. Ehtemam-Haghighi, **Y.J. Liu**, G. Cao, L.-C. Zhang, Phase transition, microstructural evolution and mechanical properties of Ti-Nb-Fe alloys induced by Fe addition, Materials & Design. 97 (2016) 279-286.

[9] X. Li, M. Roberts, **Y.J. Liu**, C. Kang, H. Huang, T. Sercombe, Effect of substrate temperature on the interface bond between support and substrate during selective laser melting of Al–Ni–Y–Co–La metallic glass, Materials & Design. 65 (2015) 1-6.

[10] S. Zhao, W.T. Hou, YL Hao, **Y.J. Liu,** L.C. Zhang, S.J. Li, R. Yang, Influence of annealing treatment on microstructure and mechanical properties of graded structure Ti-6Al-4V alloys, Rare Metal Materials and Engineering, In press (2017)

Acknowledgments

I would like to take this opportunity to gratefully thank those people who had supported me during my PhD study. Firstly, I would like to express my sincere gratitude equally to my supervisors, i.e. Assoc/Prof. Lai-Chang Zhang, Prof. Yulin Hao, Prof. Shujun Li and Assoc/Prof. Tim Sercombe, for providing me an opportunity to be a part of their research group where I had accessed to high-tech devices as well as meeting helpful and friendly scientists and staffs. I really appreciate all my supervisors' advices, attentions, time and supports. They always encouraged and motivated me to conduct my PhD work with a high efficiency and effectiveness. It is not really easy to thank them with words.

Also, I would like to express my special thanks to my advisor Dr. Haoliang Wang and equally to all my colleagues/friends especially Dr. Xiaopeng Li, Dr. Xiaojun Wang, Dr. Xiaoxue Xu, Dr. S. Ehtemam-Haghighi, Dr Greg Maguire, Dr Zibo Zhao, Dr. Yang Yang, Dr Shaogang Wang, Dr Jingping Cui, Wentao Hou, Zhe Jia, Peng Qin, Weijie Wang, Qinsi Xu, Shuo Zhao, Jinrui Zhang, Xin Gai, Yan Liu, Cong Li, Yue Jiang, Zheng Liu, Guowei Wang, Xiaofei Lei, Ruipeng Guo, Yiqiang Mu, Chunwei Shao, Awais Shah, Yulan Li, Suyun He, for all their supports, attentions, helpful discussions and technical assistances. In addition, I appreciate the financial support from the Projects funding scheme (DP110101653) (Australia), 863 Project (2015AA033702) (China), National Basic Research Program of China (2012CB619103, 2012CB933901) and National Natural Science Foundation of China (51271182, 51271180) for my PhD study. I also appreciate the ECU Postgraduate Scholarship (ECU-PRS) (International) which has assisted in minimizing my living and study expenses, while allowing me to focus on the most important thing i.e. completing my PhD.

Finally, I am extremely grateful to my wife (Yuting Liu) for her constant supports, love, affection and sacrifices. I dedicate my PhD thesis to her.

1. Introduction and background

1.1 Introduction

With new technology and a high economic value of new carrier materials, materials science and technology is being developed in new areas. Biomedical materials are novel high-tech materials used to diagnose, treat, repair or replace diseased tissues, organs, or functions of living organisms [1]. Biomedical materials mainly study their biocompatibility, implants and hard tissue reaction, the cytotoxicity, the relationship of the basic structure and characteristics. In addition, durability, corrosion resistance and surface modification are also increasingly important [2]. It intends to diagnose, treat or replace human tissue or organs, or enhance how they function.

Nowadays, a target of researchers is to develop implants that work for longer periods of time, or for an entire lifetime, without failure or the need for revision surgeries [1]. This requires a service period of at least 15 to 20 years for older patients, and more than 20 years for younger patients. Excellent biocompatibility, as well as a low modulus of elasticity and no cytotoxicity, is indispensable, especially in load-bearing applications [1]. Moreover, implant materials should have enough mechanical strength to sustain the loads to which they are exposed, so that they do not undergo fracture. So far, stainless steel, CoCr alloys and titanium alloys are three most common metallic biomaterials. However, compared to CoCr alloys and stainless steel, titanium and some of its alloys are most preferred to orthopaedic applications due to their unique properties, including low density, high strength and good biocompatibility.

The key for implant applications is a low elastic modulus, though fatigue resistance and high strength are also very important factors. Ti2448 was first reported in 2005 [3]. This alloy is a new generation of β-type biomedical grade titanium alloy that has the potential to provide significant improvements as an implant material. So far, the only alloy with a 42-50 GPa modulus is titanium, with the lowest initial Young's modulus [3]. Even so, the Ti-24Nb-4Zr-8Sn alloy has a modulus at least an order of magnitude larger than bone with a Young's modulus range from 1 GPa to 30 GPa. A mismatch of modulus between a Ti2448 alloy implant and the surrounding bone tissue might lead to stress shielding, which eventually causes bone resorption. This situation has been identified as a main reason for implant loosening [4, 5]. The modulus of a biomaterial can be reduced by introducing porosity, which, provided the porosity is interconnected, can have the additional desired effect of promoting bone in-growth [6, 7, 8], along with easy diffusion of nutrients to and waste from the implant [9, 10].

AM is an emerging manufacturing technology which creates parts using additive processes, rather than the more traditional subtractive techniques. While there are a number of different technologies which fall under the AM umbrella (including SLM and EBM) they are all layer-wise techniques. In essence, energy and/or material are delivered to a point to produce a solid. A series of lines are then traced out to make a layer and a series of layers formed to make a three dimensional part. AM is most widely used in the transport and consumer products industries but has been found positive application in medicine, forensics, architecture, robotics and the cinema. AM is also one of the most advantageous methods for fabricating the complicated structure of an artificial bone implant. It is possible to obtain an ideal implant by combining the new generation Ti2448 alloy with the most advantageous manufacturing method. However, the parameters of AM manufacturing are hard to explore, and they can affect mechanical properties including microstructure, tensile stress, compressive stress, fatigue property, hardness, density and fracture morphology.

Therefore, an understanding of the process mechanisms and effects of process parameters is significant for the future development of implants. The purpose of this thesis is to improve the properties of Ti2448 porous structures using AM (including

SLM and EBM systems) base for tuning the Ti2448 manufacturing parameters, which include input energy, scanning track, scanning speed, and then to observe the microstructural characterisation and to analyse the mechanical properties.

1.2 Research highlight and methods

AM provides an opportunity to proceed directly from computer model to finished part without tooling or machining. Without tooling, the time and cost of moulds and dies are eliminated and the design constraints consequent on the geometric limitations imposed by the tool are removed. AM is clearly a major technology with wide applicability that continues to develop and grow. AM-produced titanium components have attracted researcher’s attention due to their advantages including high strength, corrosion resistance and low modulus [11, 12]. This thesis presents the manufacturing parameters of AM-produced beta-type porous titanium components and their extremely low modulus, good super-elastic and great fatigue properties.

The objective of this thesis is to develop the science that will underpin a new generation of bone implants with porous structure. The main work in this project will focus on the extensively used Ti2448 alloys in the medical field, using SLM and EBM approach to manufacture the Ti2448 porous structure with low Young’s modulus. Firstly, this research will obtain the high relative density porous structure by optimizing the SLM and EBM process parameters. Furthermore, it observes the morphology of the SLM- and EBM-produced structures strut surface and defect poor distribution inside the strut, then analyses the reason of the roughness of the strut surface and defects formation. In addition, the relationship between the microstructures and mechanical properties, which include the hardness compressive, Young’s modulus and fatigue properties, will be studied. The completion of this thesis will provide significant research purpose in mechanical property of porous materials as well as can optimize the design of porous titanium or titanium alloys and establish theoretical fundamental to actual application in biomedical field. This project will break through some key technologies in the aspects of porous alloy preparation and porous structure to develop new generation bone repairing materials to satisfy ultrasonic orthopedic clinical technology. This purposed porous material will implement the medical implant application and development. The batch production capacity and pre-clinical evaluation of the purposed porous material will be highly concerned.

1.3 Reference

[1] M. Long, H. Rack, Titanium alloys in total joint replacement—a materials science perspective, Biomaterials. 19 (1998) 1621-1639.

[2] V. Karageorgiou, D. Kaplan, Porosity of 3D biomaterial scaffolds and osteogenesis, Biomaterials. 26 (2005) 5474-5491.

[3] Y. Hao, S. Li, S. Sun, C. Zheng, Q. Hu, R. Yang, Super-elastic titanium alloy with unstable plastic deformation, Applied Physics Letters. 87 (2005) 091906-091906-091903.

[4] W.C. Head, D.J. Baulk, R.H. Emersom, Titanium as the material of choice for cementless femoral components in total hip arthroplasty, Clinnical Orthopaedics and Related Research. 311 (1995) 85.

[5] D.M. Robertson, L. St. Pierre, R. Chahal, Preliminary observations of bone ingrowth into porous materials, Journal of Biomedical Materials Research. 10 (1976) 335-344.

[6] S.F. Hulbert, S.J. Morrison, J.J. Klawitter, Tissue reaction to three ceramics of porous and non-porous structures, Journal of Biomedical Materials Research. 6 (1972) 347-374.

[7] C.E. Holy, M.S. Shoichet, J.E. Davies, Engineering three-dimensional bone tissue in vitro using biodegradable scaffolds: Investigating initial cell-seeding density and culture period, Journal of Biomedical Materials Research. 51 (2000) 376-382.

[8] L. Yang, O. Harrysson, H. West, D. Cormier, Compressive properties of Ti–6Al–4V auxetic mesh structures made by electron beam melting, Acta Materialia. 60 (2012) 3370-3379.

[9] S. Yue, P.D. Lee, G. Poologasundarampillai, J.R. Jones, Evaluation of 3-D bioactive glass scaffolds dissolution in a perfusion flow system with X-ray microtomography, Acta Biomaterialia. 7 (2011) 2637-2643.

[10] C.M. Murphy, F.J. O’Brien, Understanding the effect of mean pore size on cell activity in collagen-glycosaminoglycan scaffolds, Cell Adhesion & Migration. 4 (2010) 377-381.

[11] H. Attar, K.G. Prashanth, A.K. Chaubey, M. Calin, L.C. Zhang, S. Scudino, J. Eckert, Comparison of wear properties of commercially pure titanium prepared by selective laser melting and casting processes, Materials Letters. 142 (2015) 38-41.

[12] L. Thijs, F. Verhaeghe, T. Craeghs, J.V. Humbeeck, J.-P. Kruth, A study of the

microstructural evolution during selective laser melting of Ti–6Al–4V, Acta Materialia. 58 (2010) 3303-3312.

2. Literature review

2.1 Biomaterial

2.1.1 Introduction

A biomaterial is a nonviable material used in a medical device that is intended to interact with biological systems. Biomaterials have been attracting highly attention for human health, and much progress has been made during the last decade. The application of biomaterials enhances the fineness and longevity of human life. Growth in the biomaterials field is accelerating [1, 2]. The field of biomaterials was recognized after the first meeting was held on biomaterials at Clemson University in Southern California in 1969. Since then, it had continuously been attracting in a great deal of attention [1]. Biomaterials are commonly defined as synthetic or natural materials that can be used in human health applications to perform a body function or replace a body part or tissue. They are used to augment, repair or replace any tissue, organ or function of the body that has been lost through trauma, disease or injury [2]. Hard tissue implants often play an essential role. It is estimated that by 2030, total hip replacements and knee arthroplasties will increase by 174% and 673%, respectively, from current rates [3]. This is due to degenerative diseases such as osteoarthritis, osteoporosis and trauma, which lead to pain or loss of function in human joints [3]. The degenerative diseases lead to degradation of the bone’s mechanical properties as a result of the immoderate loading or absence of normal biological self-healing processes [3].

The target of researchers is to develop implants that work for longer periods of time, or for an entire lifetime, without failure or the need for revision surgeries [4]. This requires a service period of at least 15 to 20 years for older patients, and over 20 years for younger patients [5]. Consequently, developing the implant materials with superior corrosion resistance in the body environment, excellent biocompatibility and a low modulus of elasticity and without cytotoxicity is indispensable, especially for load-bearing applications [1]. Implant materials should have enough mechanical strength to sustain the loads to which they are exposed so that they do not undergo fracture. Furthermore, a bio-implant should possess a high wear resistance in the corrosive body environment, in addition to fatigue strength and fracture toughness [5]. The low wear resistance leads to the release of wear debris in the surrounding tissue [1]. The resultant wear debris initiates inflammatory reactions that lead to osteolysis. Finally, this results in implant loosening, as the bonds between the bone and implant are destroyed due to the body's attempts to digest this wear debris.

2.1.2 Type of biomaterial

In general, physical properties are the main factors to consider when an implant is designed. So far, the three most widely used biomaterials for implants are polymers, ceramics and metallic biomaterials. All three common biomaterials must meet the following requirements:

- A biocompatible chemical composition to avoid adverse tissue reactions
- Excellent resistance to material degradation (e.g., corrosion resistance for metals, or resistance to biological degradation in polymers)
- Acceptable strength to sustain the cyclic loading endured by the joint
- A low modulus to minimize bone resorption
- High wear resistance to minimize wear debris generation

The applicability of various material types in orthopaedic and maxillofacial surgery largely depends on their mechanical properties. Fig. 2.1 lists the requirements of implants. It is shown that metallic materials are suitable for bearing virtually every kind of load, depending on their specific properties, while ceramics can only be highly loaded by compression stresses.

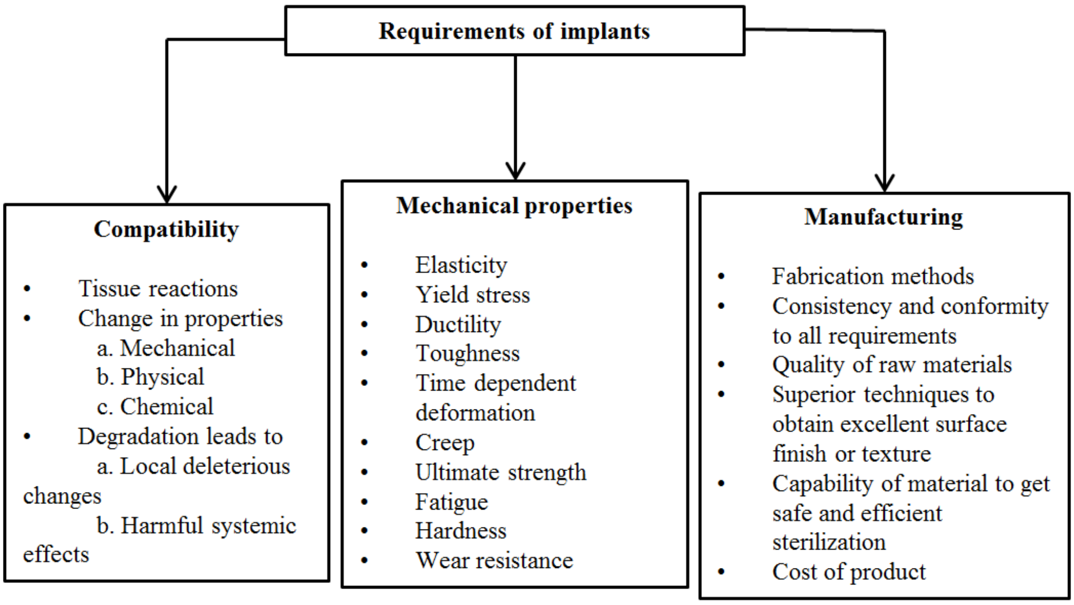

Fig. 2.1 Implant requirements in orthopaedic applications.

2.1.2.1 Polymeric biomaterials

Biomedical polymer materials include natural and synthetic, in particular, the synthetic polymer medical materials have a fastest growing. Through the molecular design, good physical and mechanical biocompatibility of biological materials can be obtained, in which soft materials commonly used in human soft tissue such as blood vessels, knuckles and other substitutes; liquid synthetic materials such as room temperature vulcanized silicone rubber can be used for injection-type tissue repair materials; synthetic hard materials used in artificial dura mater, cage spherical valves for artificial heart valves, artificial joint. There are many advantages of polymeric biomaterials, such as being able to promote cell growth, and the range of applications is broad and complex.

Applications for biodegradable polymeric materials alone include:

- Large implants, such as bone screws and bone plates
- Small implants, such as staples, sutures and nano- or micro-sized drug delivery vehicles
- Plain membranes for guided tissue regeneration
- Multifilament meshes or porous structures for tissue engineering

2.1.2.2 Ceramic biomaterials

Ceramics have been widely used in tissue engineering due to their excellent biocompatibility and biodegradability. In the physiological environment, they are able to gradually degrade, absorb and promote bone growth. Ultimately, they are capable of replacing damaged bone with new tissue. However, their low mechanical properties limit calcium phosphate ceramics in load-bearing applications. The class of ceramics used for the repair and replacement of diseased and damaged parts of the musculoskeletal system are referred to as bioceramics. In general, ceramics are mainly used as orthopaedic implants and in dental applications, and also as non-load bearing for bioactivity. Ceramics can offer the advantages of mechanical properties, but as biomaterials, they are hard [6]. This makes it difficult to use them at load-bearing sites.

2.1.2.3 Metal biomaterials

Metals designed to be applied as a substitute for bone grafts must fulfil certain requirements:

- A good corrosion resistance to avoid degradation in the biological environment
- Biocompatibility such that no toxic, injurious or allergic reactions in the biological systems occur
- Adequate mechanical properties, such as high fatigue strength and a Young's modulus similar to that of human bone, are necessary to avoid fracture and stress shielding
- For cost-saving and good process ability, materials need to be relatively easy to process by, for example, casting, deformation, welding or brazing
- The availability is an important factor in choice of a material for biomedical applications

Generally, physical properties play an important role only in the case of special functional applications, such as in heart pacemaker electrodes. Good chemical and biological properties are a prerequisite for application in orthopaedic and maxillofacial surgery. The most important mechanical properties for highly loaded implants like hip endoprostheses are fatigue strength and Young's modulus. Metals have good mechanical properties for use in load-bearing sites. Stress shielding due to a high modulus is a main disadvantage [7]. To solve this problem, titanium alloy metals with a low modulus [8] are introduced. Until now, the three most widely used metals for implants have been stainless steel, CoCr alloys and Ti alloys [9]. Compared with CoCr alloys and stainless steel, titanium and some of its alloys are preferred to be used in orthopaedic applications due to their combination of unique properties including low density, high specific strength, superior corrosion resistance, excellent biocompatibility and a low modulus of elasticity [1, 10, 11, 12].

2.2 Biomedical titanium alloys

2.2.1 Introduction

Titanium has been attracting much attention in dentistry because of its good biocompatibility and mechanical properties. Wrought forms of titanium have been used in past decades; for example, beta titanium orthodontic wires, Nitinol (Ni-Ti) orthodontic wires with a shape-memory effect and endosseous dental implants have all used titanium [13, 14]. Because it was difficult to cast with conventional methods, titanium and its alloys could not be used for artificial crowns and partial prostheses. However, with the development of casting techniques and the preference for prosthetic superstructures of titanium endosseous implants, the titanium alloys become one of the most important biomaterials [15].

2.2.2 Titanium-base alloy developments

In the past, titanium alloy has been widely used as a biomaterial. Titanium has been recognized as an element for at least 200 years. However, the commercial production of titanium did not begin until the 1950s. Titanium is the fourth most plentiful structural metal in the earth, following aluminium, iron and magnesium. Naturally, it exists as TiO_2 or $FeTiO_3$, and not in its elemental state. Today, more than ever, titanium alloy is considered to be a key material in biomaterial applications. Many studies have examined the material aspects of titanium as well as its potential for use in the replacement of body functions. In general, titanium is known to be stable over long implantation times and resistant against corrosion [16]. Two hundred years ago, titanium was isolated and named for the first time. However, the metal is not even fifty years old. Due to titanium's high affinity for non-metallic elements, it is difficult to extract pure titanium from rutile (TiO_2), the most stable form of titanium oxide, or titanium ores. Since the 1950s, titanium and its alloys have been importantly reported in the aerospace industry owing to the attractive mechanical properties and excellent corrosion resistance [83]. One of the first applications in dentistry was for machined titanium dental implants. As a substitute for the lost-wax cast technique, Andersson et al. developed the Procera system with titanium machining to fabricate unalloyed titanium crowns and fixed bridges [17].

2.2.2.1 Pure titanium

Table 2.1 Maximum impurity limits (wt%) of pure titanium [18].

Type	N_{max}	Fe_{max}	O_{Max}	C_{Max}	H_{Max}
ASTM grade I	0.03	0.20	0.18	0.10	0.015
ASTM grade II	0.03	0.30	0.25	0.10	0.015
ASTM grade III	0.05	0.30	0.35	0.10	0.015
ASTM grade IV	0.05	0.50	0.40	0.10	0.015

Pure titanium has been used in the United States and Kingdom since 1950s, and it has better corrosion resistance and tissue compatibility than stainless steel in biological media environment. However, those drawbacks including low strength and poor wear resistance limit its use for the load-bearing parts, only mainly for oral repair and carrying smaller bone replacement. Pure titanium is commercially available in four different grades (American Society of Testing and Material grades I to IV) [19], based on the incorporation of small amounts of oxygen, nitrogen, hydrogen, iron and carbon. The maximum impurity limits of grades I to IV pure titanium are listed in Table 2.1

The physical and mechanical properties of pure titanium and its alloys can be greatly influenced by the addition of small traces of other elements such as oxygen, iron and nitrogen. Table 2.2, which presents the physical and mechanical properties of grade I to IV for pure titanium and dental alloys, indicates that tiny additions to pure titanium significantly change the material properties. Table 2.2 also reveals that titanium's density, 4.5 g/cm^3, is significantly less than that of gold and CoCr alloys (18.3 and 8.5,). Table 2 also shows the elastic modulus of titanium and its alloys, which are comparable to gold, but only one-half that of a CoCr alloy.

Table 2.2 Selected physical and mechanical properties of CP (commercially pure) titanium (grade I-IV), titanium alloys and dental alloys compiled from different sources [18].

Material	Density (g/cm^3)	Elongati on (%)	Tensile strength (MPa)	Yield strength (MPa)	Elastic modulus (GPa)
cp Ti(Grade I)	4.51	24	240	170	100
cp Ti(Grade II)	4.51	20	340	280	100
cp Ti(Grade III)	4.51	18	450	380	100
cp Ti(Grade IV)	4.51	15	550	480	100
Bone	0.7	1	140		2.4

In 1977, Waterstratt noticed the feasibility of casting titanium alloy for dental applications. Many studies have followed his work to examine the development of casting machines, suitable investment materials and the precise technique of dental prostheses [10].

Titanium's high affinity for oxygen, especially at elevated temperatures (above 600°C), results in being made by the casting procedure is very complicated. It requires special melting methods, investment materials and equipment to prevent metal contamination. In addition to reactions with environmental materials, the extremely low density of titanium, compared to conventional alloys, can cause casting difficulties, and a conventional broken-arm casting machine would not guarantee sufficient centrifugal forces for consistent and complete castings [20].

Titanium alloy has been developed as a biomaterial since the 1960s because of its excellent properties. Requirements for joint replacement continue to grow as people live longer and incur more injuries through sports or jogging, or are seriously injured in road traffic and other accidents. Light, strong and totally biocompatible, titanium is one of few materials that naturally matches the requirements for implantation in the human body. Titanium alloys are widely used in biomaterial applications because of the additional advantages of good local spot weld ability, easy shaping and finishing by mechanical and electrochemical processes [1, 10, 11].

2.2.2.2 Ti-6Al-4V, Ti-5Al-2.5Fe and Ti-6Al-7Nb alloys

Ti-6Al-4V is an alloy that was originally designed for aerospace applications [21]. Later alloys did not include V, because it has the potential to lead to diseases. In terms of cytotoxicity, vanadium is toxic in both the elemental state and as an oxide [22], and it is potentially problematic, as the reason of the element V and Al ions leached from the alloy. This could result in Alzheimer's disease, neuropathy and osteomalacia [23]. Therefore, it is important to carefully consider additions when designing new generation alloys, especially for biomedical alloys. These alloys included Ti-6Al-7Nb and Ti-5Al-2.5Fe [1]. These alloys contain non-toxic elements Nb, Fe instead of toxic elements V, eliminating the toxicity of V elements on the human side effects. Ti-6Al-7Nb ($\alpha + \beta$) alloy was developed by Switzerland SULZER Medical Technology Company in 1978. It is a good alloy for surgical implants in clinical application in 1985. It is made of dental cast materials withthe strength 2 times higher than that of the pure titanium, the mechanical properties better than the Co-Cr alloys and the finished tooth having thinner shape and lighter density than the Co-Cr alloy [24]. Although the Ti-6Al-7Nb and Ti-5Al-2.5Fe alloys have good biocompatibility and corrosion resistance, there are still many shortcomings, such as still containing the cytotoxic element Al; low biological activity, which is lower than that of bioactive ceramics. The modulus of elasticity is similar with Ti-6Al-4V alloy, and there is still a big gap with the maximum elastic modulus of human skeleton [25]. The mismatch between the elastic modulus of this implant and bone will make the load cannot be well delivered by the implant to the adjacent bone tissue, thereby generating the "stress shielding" phenomenon, resulting in implant failure. Researchers conducted research on new biomedical β-titanium alloys in order to meet the requirement of the high standard, those alloys contain advantages such as non-cytotoxicity, low elastic modulus, and high biomechanical adaptability of the alloying elements, and to improve the interface between the implant and the natural bone, to meet the higher requirements of clinical implant materials,.

2.2.2.3 New generation *β*-type titanium alloys

New generation *β*-type titanium alloys were developed with attractive properties such as a low modulus and high strength. These alloys included Ti-12Mo-6Zr-2Fe, Ti-15Zr-4Nb-2Ta-0.2Pd and Ti-13Sn-13Zr. A minimum elastic modulus was obtained in 2005 with the development of the Ti2448 alloy [8]. Ti2448 is one kind of *β*-type titanium alloy with a bcc crystal structure, and its low modulus and high compressive strength makes it to be the ideal biomaterial for fabricating new generation implants with fewer stress-shielding problems [8]. So far, Ti2448 has the lowest initial Young's modulus compared to any titanium alloys. It is one of the bionic human skeletal characteristics of the new biomedical metal materials. The alloy has plenty of advantages, such as high strength, high damping, super elasticity and excellent performance. It has such excellent properties because it stems, in part, from the unique deformation mechanism. In the past, most of the super-elastic metal material from a stress-induced reversible martensitic transformation in a Ti2448 martensitic transformation was observed, it was the first time to be found before cannot be accomplished in metallic materials dislocation loops homogeneous nucleation and reversible movement in the low stress condition. These phenomena make Ti2448 superior to other metal materials. Ti2448 is a new generation biomaterial with a Young's modulus of 42-50 GPa and a high strength, which can reach 850 MPa [8].

With the development of titanium alloys, achievements are also obtained via comparison of conventional titanium alloys with the latest titanium alloy. Zheng *et al.* designed a test method in 24 dogs in order to compare the performance of a Ti64 half-pin with a Ti2448 half-pin. They found that the Ti2448 half-pin had greater performance than the Ti64 half-pin [26]. They observed the necrotic layer in bone formation, which was surrounding the Ti-6Al-4V half-pin (Fig. 2.2). On the contrary, the fresh bone cells grew well surrounding the Ti2448 half-pin. This is direct evidence that the Ti2448 is a better new generation biomaterial for bone implants compared to other titanium materials.

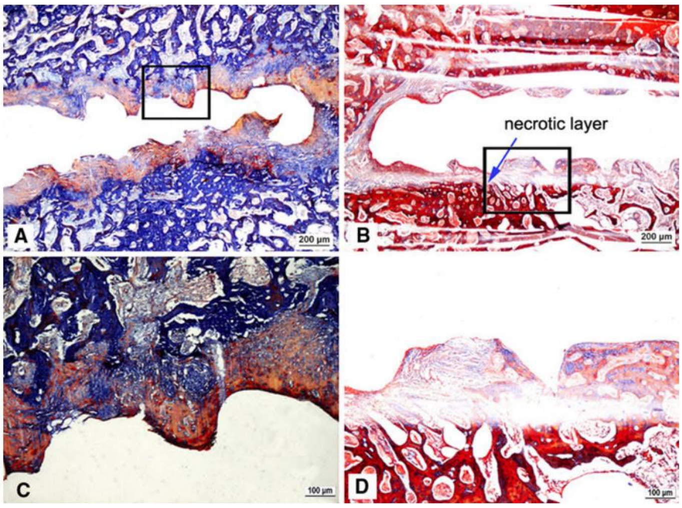

Fig. 2.2 Histological observation of decalcified pin–bone interface in group A (a, c) and group B (b, d) by modified Ponceautrichrome staining at8weeks postoperatively [26].

2.2.3 Modulus of elasticity of titanium alloys

The elastic modulus of appropriate alloys should be similar to that of cortical bone. Cortical bone, or the compact bone, is the main constituent of the human skeleton, and is essential for organ protection, support and movement. The high modulus of elasticity of conventional alloys has led to a stress-shielding effect and failure of the implants [5]. The low elastic modulus, mimicking that of bone, may minimize or eliminate stress-shielding phenomena. Stress shielding is a non-homogeneous stress transfer between the metallic implant and the bone due to am is match of stiffness. Generally, stress is transferred through the implant, as the Young's modulus of implants is much higher than that of bone. This can lead to reduction in bone density, as there is no load stimulus for the continued remodelling that is required to maintain bone mass. Under such conditions, loosening of the implant and subsequent refracturing of the bone can occur [3].

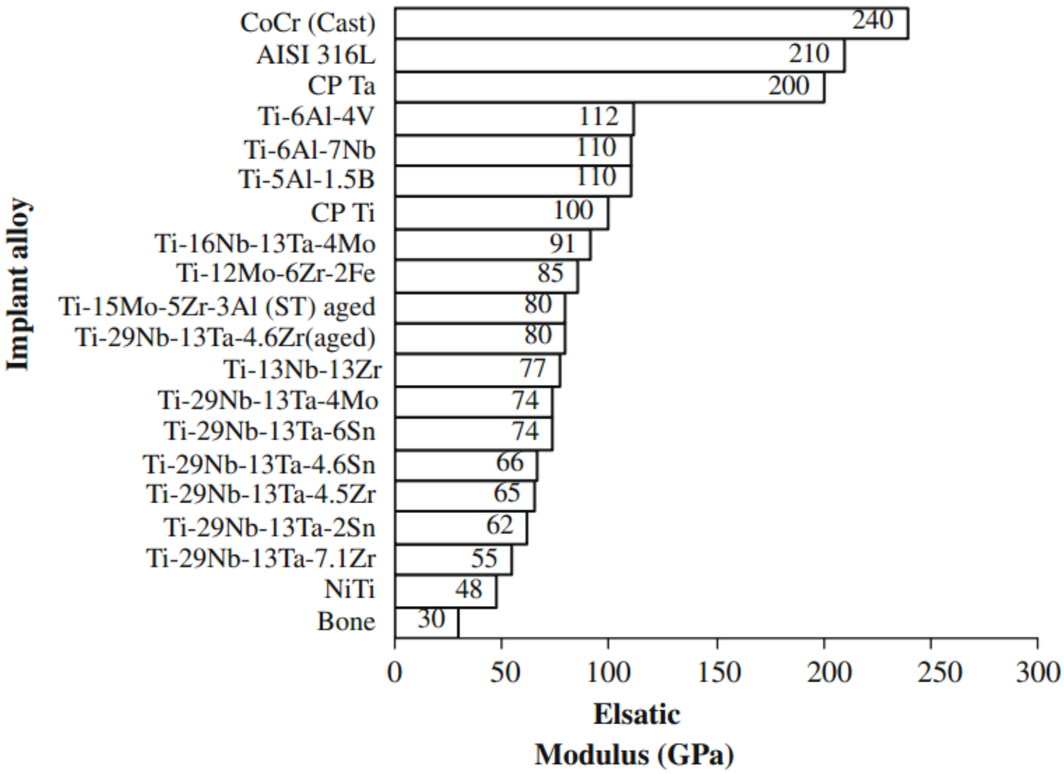

Fig. 2.3 Young's modulus of different kinds of metallic biomaterials [1].

The modulus of elasticity in titanium alloys varies from 42 to 112 GPa, which is much lower and closer to that of bone, compared to that of stainless steel 316L (210 GPa) and CoCr alloys (240 GPa). Fig. 2.3 shows the Young's modulus of biomedical alloys compared to bones. The most widely used titanium alloys are (α+β) microstructures that still have a higher modulus of elasticity than that of bone. Ti alloys are categorized into three different groups: α-, β- and (α+ β)-type alloys. Pure titanium has a hexagonal close-packed crystal structure, called α titanium, which transforms to a body cubic structure, β titanium, when the temperature is increased to 883°C. Because of its crystalline structure, the β microstructure in Ti alloys exhibits a lower elastic modulus than α- and (α+β)-type alloys. Thus, it is considered to be effective in avoiding stress-shielding phenomena, and hence, promoting bone remodelling. It is known that elements dissolved in titanium can influence this allotropic transformation temperature. The alloying elements are classified based on their effect into α-stabilizers and β-stabilizers.

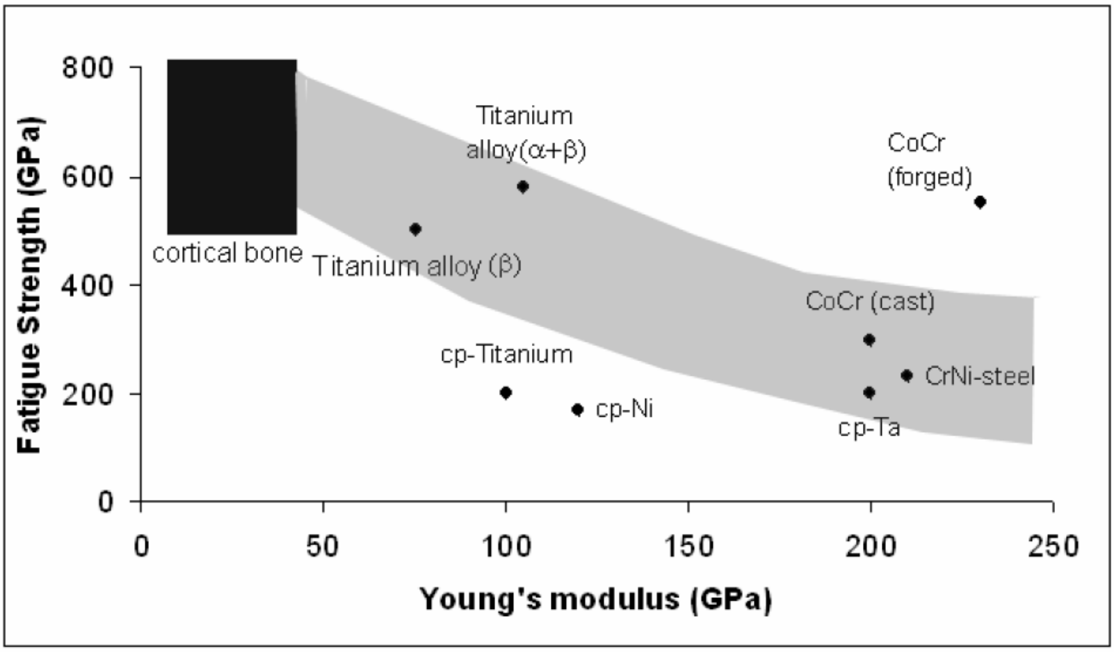

Fig. 2.4 Biofunctionality of metallic biomaterials [1].

A comparison of the biofunctionality of various alloys shows the exceptional properties of Ti and its alloys due to the low Young's modulus (Fig. 2.4). From a biomechanical point of view, it is desirable to have a Young's modulus comparable to that of bone in order to achieve a good load transfer from the implant into the bone, which leads to the continuous stimulation of new bone formation. Alloying with β-stabilizing elements can result in a further reduction of the Young's modulus of Ti alloys. For example, the alloy Ti30Ta, which belongs to the group of near β-type titanium alloys, shows a reduction of Young's modulus of 80%, as compared to CP Ti.

Most metallic biomaterials have a significantly higher density (2 to 4 times) and are much stiffer (5 to 10 times) than human bone. Too much stiffness and weight tend to create undesirable conditions, leading to stress shielding, bone resorption and atrophy. The density of Ti and its alloys is significantly lower than that of other metallic materials (Fig. 2.6), making Ti-based implants lighter than similar implants made of stainless steel or CoCr alloys.

Until now, most Ti-based implants have been used in dense form, although dense forms may lead to problems, such as interfacial instability within host tissues, a biomechanical mismatch of elastic constant and a lack of biological anchorage for tissue in-growth [33,34]. In general, joint replacement failure is rarely due to the mechanical failure of materials, such as fatigue fracture of the implant. Aseptic loosening of the implant is a more common cause of arthroplasty failure. This occurs several years after the implant has been in situ and functioning reasonably [11]. In addition to sufficient mechanical properties, highly loaded endosseous implants like hip endoprostheses require a good load transfer from the implant into the bone in order to stimulate the formation of new bone, which leads to a good long-term implant integration.

2.2.4 Tensile properties of titanium alloy biomaterials

A tensile specimen is a standardized sample cross-section. It has two shoulders and a gauge (section) in between. The shoulders are large, so they can be readily gripped, whereas the gauge section has a smaller cross-section, so deformation and failure can occur in this area (Fig. 2.5).

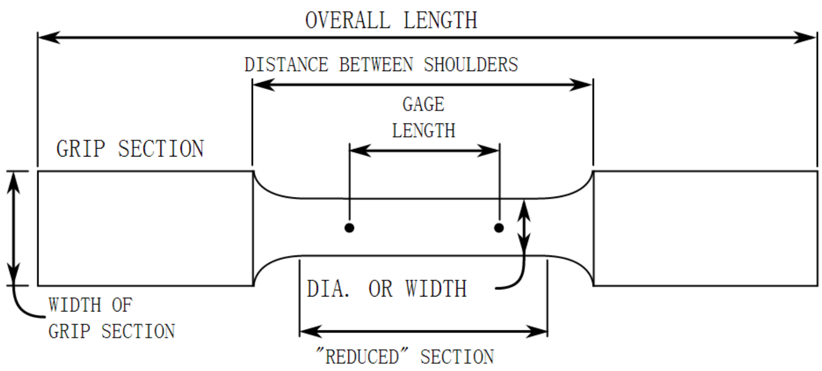

Fig. 2.5. The tensile specimen structure.

Table 2.3. The tensile properties of titanium for biomaterial applications.

Alloy	Tensile strength(MPa)	Yield strength(MPa)	Type of alloy
Pure Ti grade 1	240	170	α
Pure Ti grade2	345	275	α
Pure Ti grade 3	450	380	α
Pure Ti grade 4	550	485	α
Ti–6Al–4V ELI	860-965	795-875	α+β
Ti–6Al–4V	895-930	825	α+β
Ti–6Al–7Nb	900	880-950	α+β
Ti–5Al–2.5Fe	1020	895	α+β
Ti–5Al–1.5B	925	820-930	α+β
Ti–15Sn–4Nb–2Ta–0.2Pd	1109	790	β
Ti–15Zr–4Nb–4Ta–0.2Pd	919	806	β
Ti–13Nb–13Zr	973	836	β
Ti–12Mo–6Zr–2Fe	1060-1100	100-1060	β
Ti–15Mo	874	544	β
Ti–15Mo–5Zr–3Al	852	838	β
Ti-15Mo–2.8Nb–0.2Si	979	945	β
Ti–35.3Nb–5.1Ta–7.1Zr	596.7	547	β
Ti–29Nb–13Ta–4.6Zr	911	864	β

Due to the attractive properties of titanium alloys, the alloys are expected to be much more widely used for implant materials compared to other metallic implant materials.

The titanium alloys can be displayed via a tensile test performance. The tensile properties of titanium are listed in Table 2.3. The yield strengths of titanium alloys are mostly distributed within the range of 500-1000 MPa. The properties of titanium alloy can lead to excellent performance when they are manufactured by SLM. Zhang et al. [7] have shown the typical stress-strain curves of the samples built by SLM at different laser speeds (Fig. 2.6). All specimens showed an ultimate tensile strength of ~660MPa.

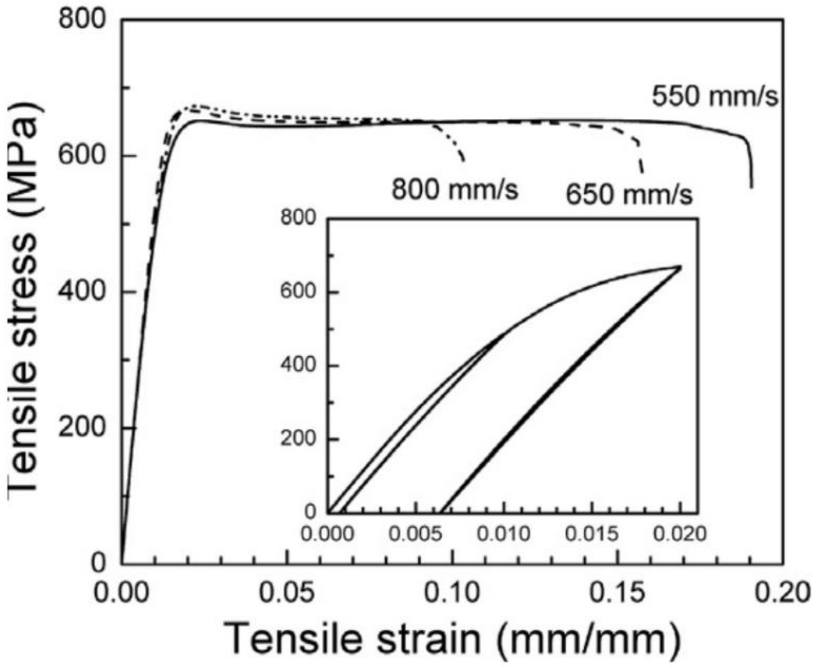

Fig. 2.6 Typical stress–strain curves of parts processed at laser scan speeds of 550, 650 and 800 mm/s [7].

2.2.5 Corrosion behaviour of titanium alloy biomaterials

Metals and alloys are degraded by electrochemical attacks when they are exposed to the body’s hostile environment. The aggressive aqueous medium in the human body includes various anions, such as chloride, phosphate and bicarbonate ions. Due to cothodic and anodic reactions, the metallic components of the alloy are oxidized to their ions, and the dissolved oxygen is reduced to hydroxide ions. Metallic implants that are corrosion resistant are in a passive state. Passive metals have a thin, compact oxide layer on their surface that separates the release of ions. This release may cause allergic and toxic reactions in the body [5]. Titanium derives its excellent corrosion resistance due to the rapid formation of a stable self-protecting oxide layer on its surface. This layer is composed mostly of TiO_2. When the surface oxide film of the implant materials is broken and exposes the metal underneath, corrosion proceeds and metal ions are released continuously unless the new film is reformed. The time required for oxide film reformation or repassivation is different for various materials [1].

2.3 Biomaterials' porous structure

2.3.1 Introduction

It is very important to study a bone's information before introducing an artificial implant. The primary structural function of bone and its limited capacity for self-regeneration has made it a common target for tissue engineering research, with over 3000 papers published over the last 25 years investigating bone tissue engineering scaffolds. Although the perfect bone tissue engineering scaffold has remained elusive, this body of work has identified the key properties required [27, 28]. The unique mechanical performance of natural bone is characterized by high toughness, high specific strength and low stiffness. Porous metallic materials, which contain numerous advantages such as low density, high porosity, large specific area, low Young's modulus, good strength and excellent energy absorption, have great potential for biomedical implants. Porous scaffolds are central to hard tissue engineering strategies because they provide a 3D framework for delivering reparative cells or regenerative factors in an organized manner to repair or regenerate damaged tissues [29].

The porous materials have the characteristics of low density, high air permeability, high specific surface area and high damping property, so they not only have the unique properties in the thermo acoustic and magnetic field, but also play a significant role in the lightweight and buffer vibration fields. Owing of their excellent properties, porous materials have become new engineering materials with great applications potential both in power and structure fields. Recently, these applications including aerospace, medical environmental protection petrochemical metallurgy machinery and construction industry, can be used for filtering, muffler insulation shunt packaging shielding biological transplantation, electrochemical process and many other occasions, causing increasing domestic and foreign material researchers attention. With the deepening of their research, porous materials processing preparation and performance have also been great development.

2.3.2 Porous structure properties

The porous metal is usually elastoplastic. Fig. 2.7 shows the curve comparison of metal bulk and porous structure under the tensile and compressive stress. Porous structure exhibits a slight linear elasticity.

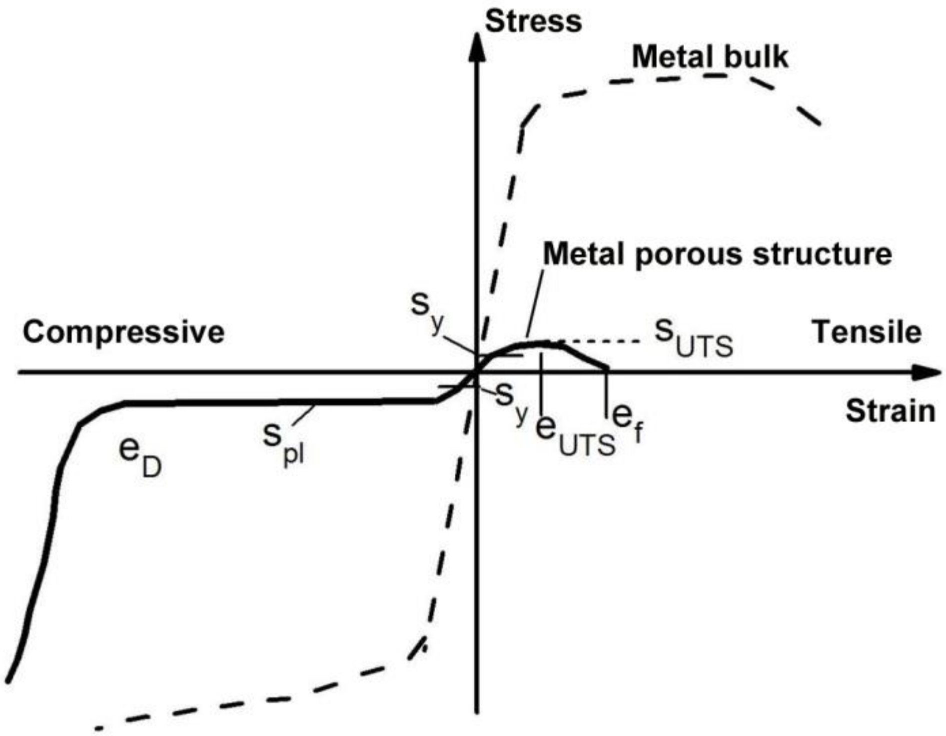

Fig. 2.7 A comparison of the stress-strain curves between the metal solids and the porous structure [30].

In order to provide a modulus comparable to that of compact (10–15 GPa) and cancellous bone (0.5–5 GPa), porous implants are required. Provided that interconnected porosity exists, scaffold structure can have the additional desired effect of promoting bone in-growth [31, 32, 33], as well as facilitating the easy diffusion of nutrients to and waste from the implant [34, 35]. Reduction of the Young's modulus as a function of porosity can be calculated by means of the equation (1):

$$Ep = E_0 (p)3/2 \qquad (1)$$

where E_p is the Young's modulus of the porous sintered material, E_0 is the modulus of the bulk material and p is the porosity. Alumina ceramics, even with a porosity of 40%, cannot result in a modulus comparable to that of bone. In contrast, Ti shows a low Young's modulus that is close to that of bone, even with relatively low values of porosity.

The most basic requirement for a successful bone tissue scaffold is that the material used exhibits osteoconduction, allowing for the direct growth of bone against the scaffold material without provoking an immune response. Bone tissue is able to grow up to and against an osteoconductive surface, but when osteoblasts laying down new bone tissue reach the surface, they are boxed in and inevitably die, leaving a thin space separating the bone tissue from the implant material [36]. This gap fills in with fibrous tissue or, worse, remains an open space, leading to implant non-union, loosening and, possibly, failure [36, 37]. Bioactive materials are able to recruit osteoblast progenitor cells from the surrounding tissue and direct them to produce new bone tissue directly onto the material [36]. Direct apposition of bone tissues on the implant surface prevents the formation of a fibrous tissue layer, and results bone-implant bond in much stronger and more durable. The key indicator of this type of surface is the presence of a cement line at the bone-material interface, which is the same feature that separates newly formed bone with older adjacent bone tissue [36]. The body is essentially treating the implant surface as it would any other bone tissue surface. Osteoconduction in a scaffold is achieved though material selection and the design of the scaffold architecture. At minimum, the material must allow for protein adsorption and cellular attachment. Ideally, the material is bioactive, allowing for direct apposition of new bone onto the scaffold surface. The scaffold must also have sufficient pore volume, size and interconnectivity to allow for vascularisation, nutrient transport and eventual bone in-growth. A scaffold meeting these requirements would exhibit high permeability and sufficient mechanical properties to prevent the crushing of the porous scaffold structure prior to tissue in-growth. Some materials are also osteoinductive, inducing and accelerating bone growth at sites within the scaffold itself, in addition to the bone-scaffold interface. By definition, osteoinductive materials are able to induce bone tissue in ectopic sites without any direct bone-to-implant contact. In practice, this definition is problematic, as there are large differences in behaviour between species and anatomical sites [38]. Bone morphogenic proteins (BMPs) are the most studied osteoinductive materials, and have been extensively used clinically [39]; but other materials, such as hydroxyapatite, can also exhibit limited osteoinductive capability [40]. A strongly osteoinductive bone tissue engineering scaffold would potentially result in accelerated bone growth and faster healing than would occur otherwise. A material is considered osteogenic if it is capable of producing bone tissue itself (i.e., through an included cellular component). The degree of osteogenic activity can be influenced by anyosteo inductive signals the scaffold contains, and varies widely depending on the anatomic site and the origin of the cells themselves.

2.3.2 Bone formation in the pores of bone and artificial scaffolds

A bone tissue scaffold can be made to be osteogenic through the incorporation of pre-seeded cells into the scaffold, or the inclusion of strongly osteoinductive signals such as BMP, which recruits native cells into the scaffold to initiate bone formation. Note that an autograft meets all of these requirements. Autografts form a strong and seamless union with adjacent bone tissue, contain proteins and cellular signals that encourage bone growth in the defect space and include living osteoblasts capable of generating new bone tissue. Introducing pores into a material structure decreases the stiffness values such that they are close to that of real bone, which can subsequently provide a good load transfer and stimulate the in-growth of new bone tissue [41]. As the picture illustrates in Fig. 2.8 (a), the porosity allows fresh bone cells to grow into the real bone open porous structure, providing an adequate biological fixation. Fig. 2.8 (b) shows the bone cells growing into the pores of a scaffold implant, creating a highly convoluted interface [42]. In Fig. 2.8 (b), white is the bone image, and blue is the scaffold.

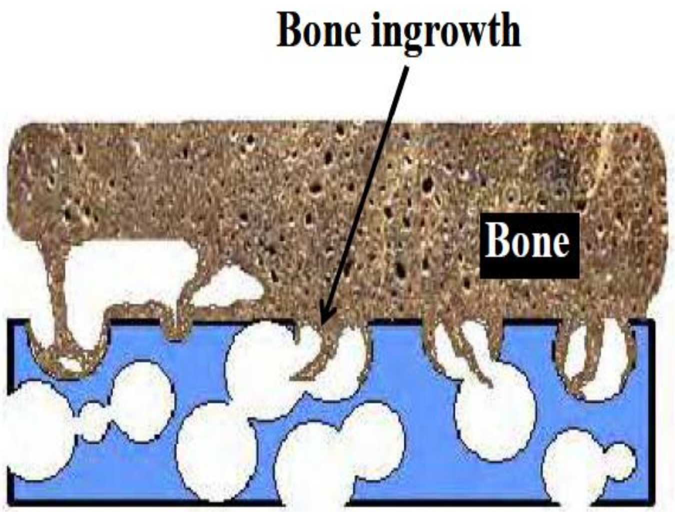

(a)

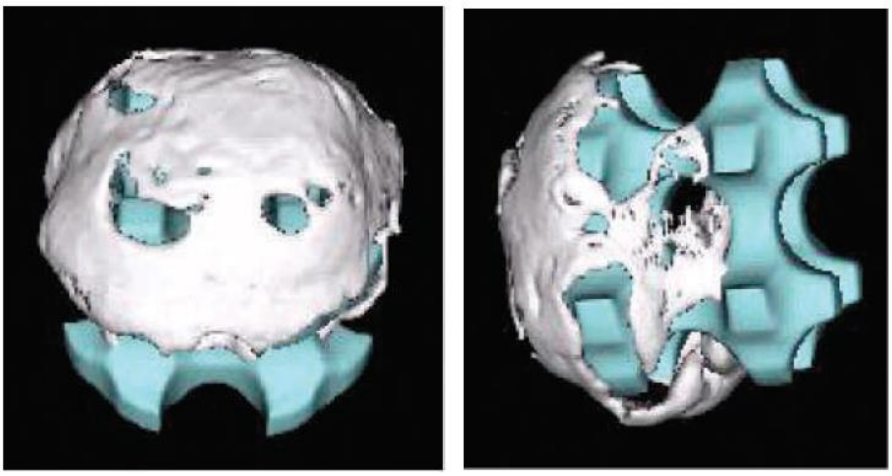

(b)

Fig. 2. 8 The pictures show bone formation in the pores of scaffolds (a)[43], and (b)[42].

2.3.3 Scaffold structures

Numerous attempts have been made to find a general-purpose replacement for bone tissue including many different kinds of scaffold structures. Although the evidence is somewhat conflicting, there is a general consensus that the ideal pore size for bone tissue in-growth into a scaffold is between 100–500 μm [44]. The pores themselves must be interconnected, with pore interconnections of at least 50–100 μm in diameter to allow for eventual vascularisation of the scaffold [45]. Smaller or less connected pores will restrict nutrient supply, resulting in necrotic regions within the scaffold and slow or no healing. In extremely soft materials, such as freeze-dried collagen scaffolds, these size requirements may be less strict, as collagen scaffolds with a pore size under ~100 μm have shown good tissue in-growth and healing response [46]. Permeability is an easily measureable property of the bulk scaffold that reflects the overall 'accessibility' of the pore space. Originally developed as a measure of fluid flow in geological applications, permeability measures the resistance of a material to fluid flow.

Several recent studies have identified permeability as a predictive factor for scaffold integration with the surrounding tissue. The success or failure of autografts used to repair a rabbit femoral segmental defect was predicted by the graft permeability measured prior to implantation [47]. In contrast, the graft size, shape, porosity and mineral content were not significant predictors of graft success. Similarly, a detailed micro-computed tomography (μ-CT) examination of bone tissue formation within sintered calcium phosphate or alumina scaffolds implanted in a trabecular defect in the proximal tibia of rabbits demonstrated that the chance of a pore containing mineralized tissue greatly increased if the minimum throat diameter between the pore and the scaffold exterior was greater than ~100 μm [45]. Permeability (and pore interconnectivity) has only been recently recognized as an important property of bone tissue scaffolds; much work remains to be done in this area.

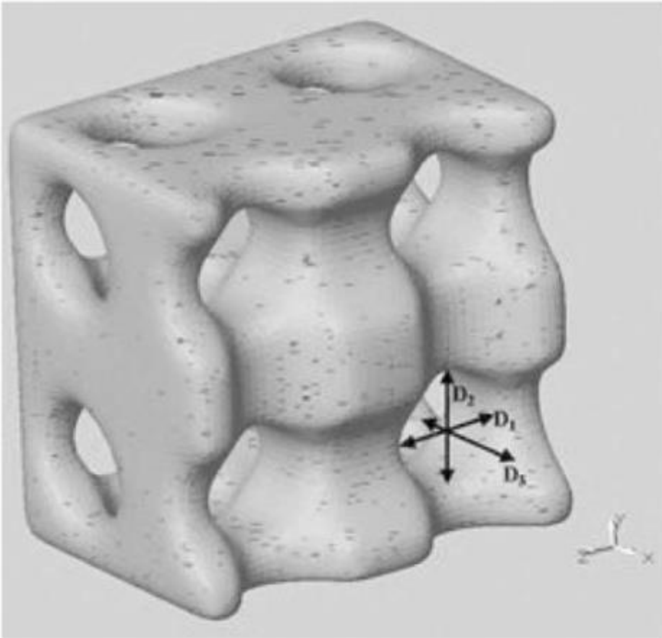

Fig. 2.9 The image of a scaffold unit with pores designed by a computer and in-grown bone cells [48].

Hollisteret al. used the functional relationship of Matlab to design the scaffold structure seen in Fig. 2.9 This example was built using the SFF method. The example test results showed agreement between native bone properties and designed scaffold properties [48].

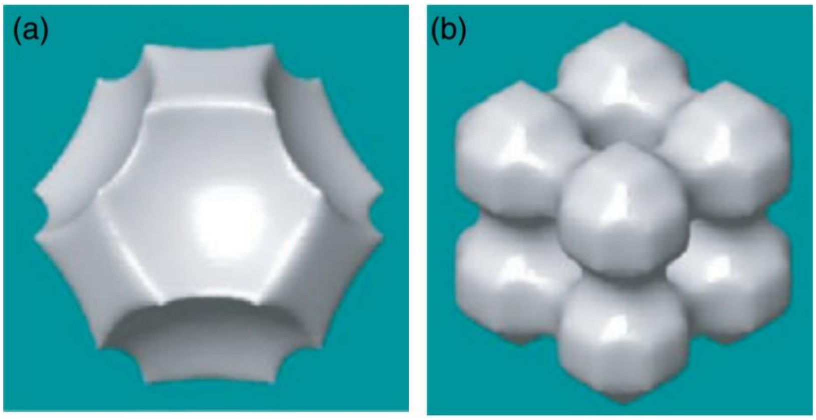

Fig. 2.10 Architectural design of scaffold unit based on geometric equations[49].

In addition, Hollister et al. designed another two-structure scaffold model, shown in Fig. 2.10. The range of pore size in interconnecting porous cylinders (Fig. 2.10 (a)) and interconnecting porous (Fig. 2.10 (b)) is from 300 μm to 1200 μm. Compressive tests showed that the modulus ranged from 0.05 GPa to 2.9 GPa, and the maximum compressive strength reached 56MPa.

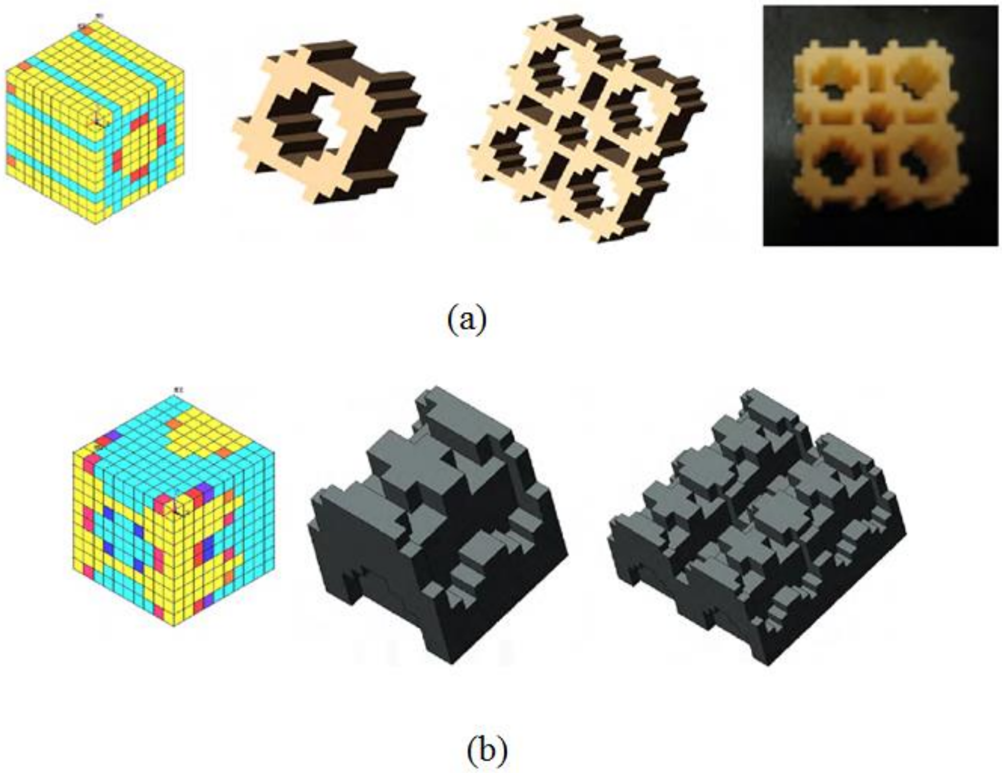

Fig. 2.11 Picture of 50% porosity scaffold structure using additive technologies [50].

Almeida and Bártolo presented a novel scaffold design based on additive technologies (Fig. 2.11). Using this method, they presented the best use of material for an implant that is subjected to either a single load or multiple load distribution. In addition, the scaffold structure lacked integrity for porosity levels higher than ±70%.

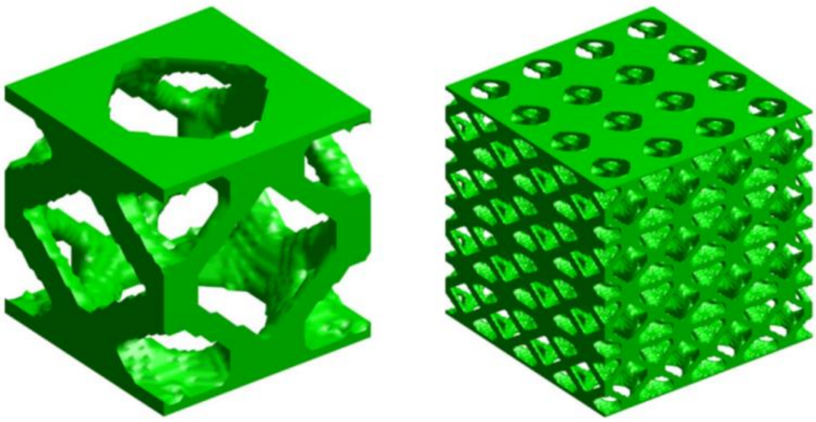

(a) (b)

Fig. 2.12 Scaffold unit and structure by using solid freeform fabrication (SFF) for researching the relationship between the stiffness and remodelling in (a) the unit of scaffolds and (b) a scaffold base cell in a 4×4×4 structure [51].

Sturm studied a numerical method, and discovered that different stiffness can lead to different remodelling results [51]. He employed the base-cell model (40×40×40 8-node hex elements) to test bone remodelling at different stages from 1 to 30 days (Fig. 2.12). His study showed that the stiffness can be affected by the percentage of porosity of the scaffold structure implants. The matching mechanical property worked best in 50% porosity scaffolds. In addition, the paper indicated that the growth of load-bearing tissue could be related to the diffusion of oxygen in a scaffold implant. Ryan [52] reported a titanium structure, which is shown in Fig. 2.13. The sample was built in a high vacuum condition. The temperature was around 1200 ° for one hour in order to fabricate the sample. Compressive strength tests revealed up to 80 MPa for a 60% porosity titanium structure. Ryan confirmed that there are some factors that affect the property of this kind of structure: melting temperature, compaction pressure and slurry concentration.

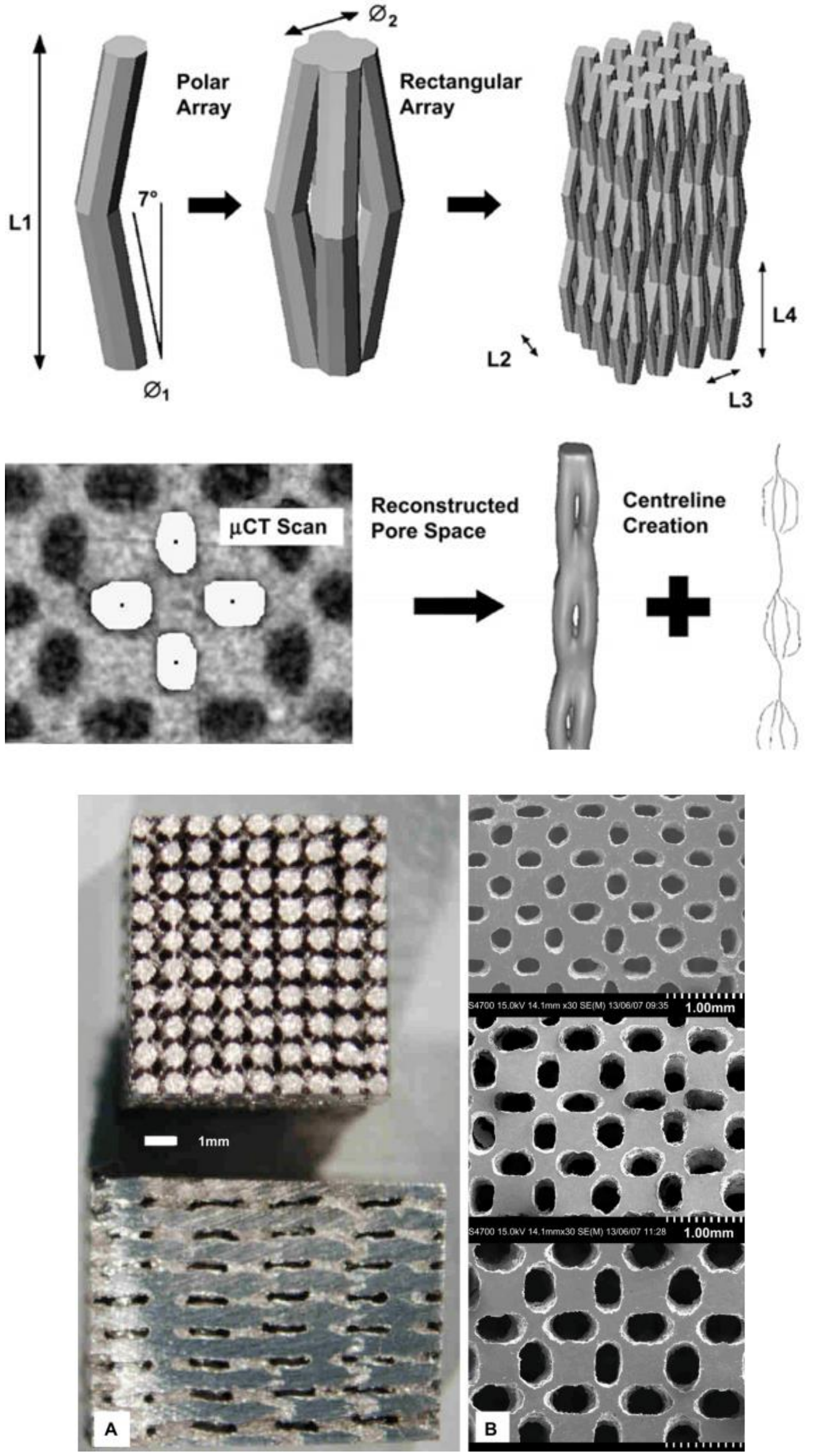

(a) (b)

Fig. 2.13. 60% porosity scaffold template model and titanium scaffolds with 200μm to 400μm pore size [52].

2.4 Additive manufacturing

2.4.1 Introduction

Mismatch of the module between the biomaterial implant and surrounding bone can cause stress shielding in the bone. This problem has been considered as a main reason for implant loosening [53]. The nature of orthodontics and orthopaedic implants requires a process to build complex and highly customisable implants to suit each patient. This is the reason why AM has a rather large market share in the biomedical sector, although the aerospace and automotive industries have begun to show some interest in AM. AM is one of the most advantageous methods for fabricating the complicated structure of an artificial bone implant. It is possible to obtain an ideal implant combining low Young's modulus titanium alloy (Ti2448) and the most advantageous manufacturing method. However, the parameters of AM manufacturing are hard to explore. The purpose of this project is to improve the properties of Ti2448 implants by changing the manufacturing parameters using SLM.

Numerous researchers studied and investigated porous materials, such as porous ceramics, polymers, and metals, in the early 1970s. In the past thirty years, AM has increased in the high-tech manufacturing industry. Since this technique can create products with complex structures, it can be regarded as a design-manufacture process with high flexibility. Although this project deals with SLM and EBM, which are two exciting and advanced AM process, a brief introduction and history of rapid manufacturing, or rapid prototyping, will be provided.

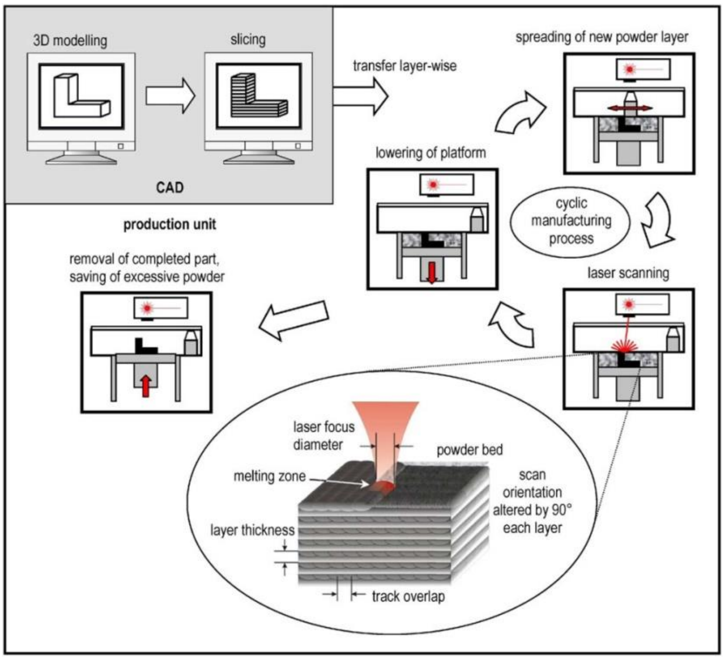

Fig. 2.14 Schematic illustrating the additive manufacturing process [54]

AM is defined as 'the use of a computer aided design based automated additive manufacturing process to construct parts that are used directly as finished products [55]. AM processes create components in a layered manner; the CAD model of a component is created and layered or 'sliced' into often thin, horizontal sections (Fig. 2.14). To prevent further confusions, from this point onwards, the term AM will be solely used to refer to such technologies in this thesis. AM processes can be traced back to the late 1980s and stereolithography. Since then, many new processes have been invented and patented. Some have disappeared into obscurity, being pushed into obsolescence largely due to the advent of newer AM processes. An overview of the development of leading AM technologies can be seen in Table 2.4.

AM systems can be broadly organized into three different categories according to the type of raw material used:

- Liquid-based systems
- Powder-based systems
- Solid-based systems

Three pioneering and ground breaking AM technologies in each category that contribute to the current state of the art technology will be highlighted and briefly explained. They are: stereolithography (SLA) (liquid-based system), fused deposition modelling (FDM) (solid-based system) and selective laser sintering (SLS) (powder-based system). Table 2.5 compares various conventional fabrication methods for manufacturing porous metallic scaffolds.

Table 2.4 AM technologies, acronyms and development years [56].

Name	Acronym	Development years
Stereolithography	SLA	1986–1988
Solid Ground Curing	SGC	1986–1999
Laminated Object Manufacturing	LOM	1985–1991
Selective Laser Sintering	SLS	1987–1992
3D Printing	3DP	1985–1997

In past two decades, AM technologies have gained many footholds in several industries, particularly the bio-medical sector and the automotive and aerospace industries. Initially, AM processes were exclusively used for generating prototypes or RP. However, advancements in technology have significantly improved the quality of the components produced, and have allowed for the direct manufacturing of final usable products [57]. The key advantages of the AM process are: the ability to produce parts with virtually any geometry imaginable, allowing for geometries that were extremely hard or impossible to build with conventional manufacturing processes; the expensive and time-intensive process of tooling is eliminated, as an AM process starts at the design stage and proceeds straight into the prototyping or production stage; and the additive nature of such systems yields minimal material wastage, as the volume of material required equals the volume of the actual component, in contrast to traditional subtractive manufacturing processes, such as cutting.

Table 2.5 Comparison of various conventional fabrication methods for manufacturing metallic porous scaffolds [29].

Author	Material	Method
Oh, I.H.; Nomura, N.; Masahashi, N.; Hanada, S. (2003)	Titanium	Sintered metal powders
Martell, J.M.; Pierson, R.H.; Jacobs, J.J.; Rosenberg, A.G.; Maley, M.; Galante, J.O.(1993)	Titanium	Sintered metal fibres
Bram, M. (2000)	Titanium, stainless steel	Space-holder method
Li, J.P.; Li, S.H.; de Groot, K.; Layrolle, P.(2002)	Titanium	Replication of polymeric sponge
Ducheyne, P; Martens, M.(1986)	Stainless steel type AISI 316 and titanium.	Fibre meshes and fibre bonding
Li, B.Y.; Rong, L.J.; Li, Y.Y.; Gjunter, V.E.(2000)	NiTi shape memory alloys	Self-propagating high temperature synthesis (SHS)
Miyao, R.; Omori, M.; Watari, F.; Yokoyama, A.; Matsuno, H.; Hirai, T.; Kawasaki, T.(2000)	Titanium	Spark plasma sintering (SPS)
Groza, J.R.; Zavaliangos, A. (2000)	WC–10%Co and Fe–2%Al	Field assisted consolidation technique (FAST)
Alvarez, K.; Hyun, S.K.; Nakano, T.; Umakoshi, Y.; Nakajima, H.(2009)	Nickel-free stainless steel	Gas injection into metalmelt
Gu, Y.W.; Yong, M.S.; Tay, B.Y.; Lim, C.S.(2008)	Ti alloy and TiH2	Decomposition of foaming agents
Bobyn, J.D.; Stackpool, G.J.; Hacking, S.A.; Tanzer, M.; Krygier, J.J.(1999)	Tantalum	Templated vapor deposition
Davies, N.G.; Teisen, J.; Schuh, C.; Dunand, D.C.(2001)	Titanium	State foaming by expansion of argon-filled pores

Competition from developing countries with low-cost work forces, particularly in the manufacturing industry, exerts pressure on companies in developed countries worldwide to focus on new innovations. In Australia and most other high-wage countries, in order to tackle this increasing competition, it is essential to improve productivity through increasing the automation level, and to improve the efficiency of production processes. AM processes like SLM and EBM could contribute to a solution for this dilemma. SLM and EBM are considered to be two of the hosts of AM techniques under the realm of rapid manufacturing, and they have ability to produce complex geometries and internal cavities fuels a market demand for highly customized or individualized one-off parts. However, a state-of-the-art process like SLM does not yield production times fast enough to compete with traditional machining methods, and hence does not provide sufficient time- and cost efficiency, and is ultimately not yet suited for mass production. Current research and literature on AM processes is mostly focused on the qualification of new materials and their industrial applications. However, there is little if any research concerning AM process efficiency, so its build rate has yet to be concluded [58]. This affirms the purpose of this project: researching the optimization of the build speed of AM.

2.4.2 Selective laser melting (SLM) fabrication method

2.4.2.1 SLM description

Selective laser melting (SLM), one of the new advanced AM technologies, is a complex physical metallurgy process involving many parameters (typically including scanning speed, laser power, scan spacing, layer thickness and scanning strategy). It has the capability of manufacturing complex component with near fully density under various groups of optimized parameters. The melting process of the SLM is completed, which refers to multiple physical fields interaction, it therefore requires a comprehensive understanding of the effect of these for optimal manufacturing. Considerable effort has been expended on a wide range of materials in order to optimize the parameters, with the aim of improving density and surface quality/roughness [59, 60, 61]. For example, Zhang *et al*. [7] found that the density and hardness generally decrease with increasing laser scan speed for a new biomedical titanium alloy. Simchi [62] reported that the densification of metal powders during SLM is dependent upon the laser energy delivered to the powder bed. Brandl *et al*. [63] demonstrated that the post-heat treatment has the most considerable effect, and the build direction has the least considerable effect, upon the fatigue resistance for SLM parts. Among all the processing parameters, the effects of laser scan speed, laser power and layer thickness have been most widely studied. There has been a small amount of work focused on the effect of atmospheric oxygen content on the quality of laser-melted parts [64].

2.4.2.2 Scanning parameters and patterns

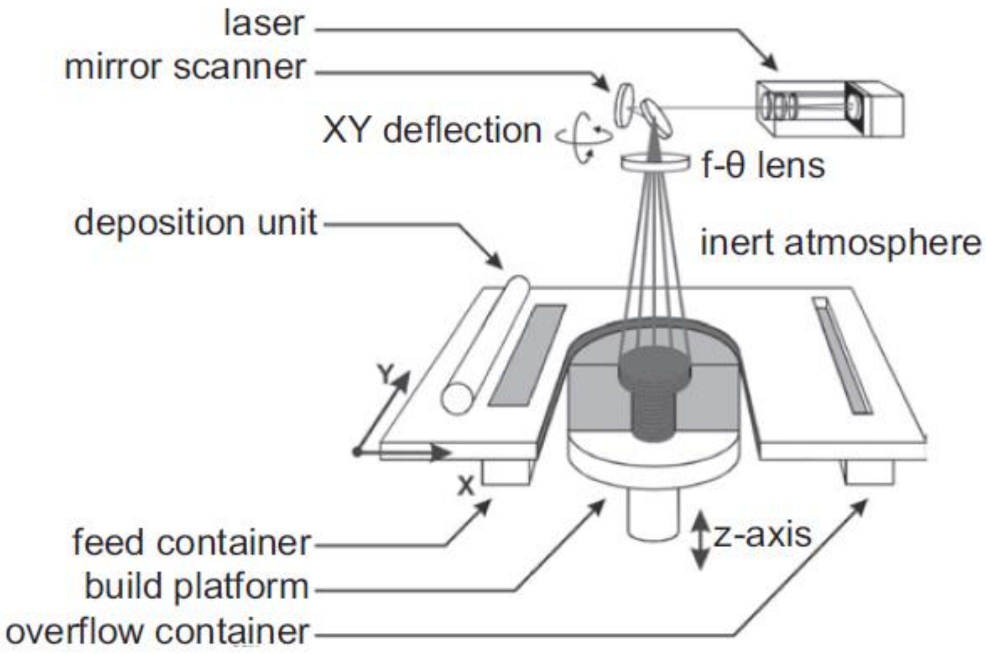

Fig. 2.15 The schematic of the SLM building process[65].

Several processing parameters, including laser power, laser speed, layer thickness, scan spacing and skin/core thickness, can be adjusted. These parameters are investigated in order to understand the effect they have on the mechanical properties of a finished part. Fig 2.15 shows the schematic of SLM scanning process. Slow scan speeds and high laser powers result in lower porosity parts due to an increase in energy density on the powder surface. This increases the local temperature, resulting in a non-linear increase in the liquid phase formation.

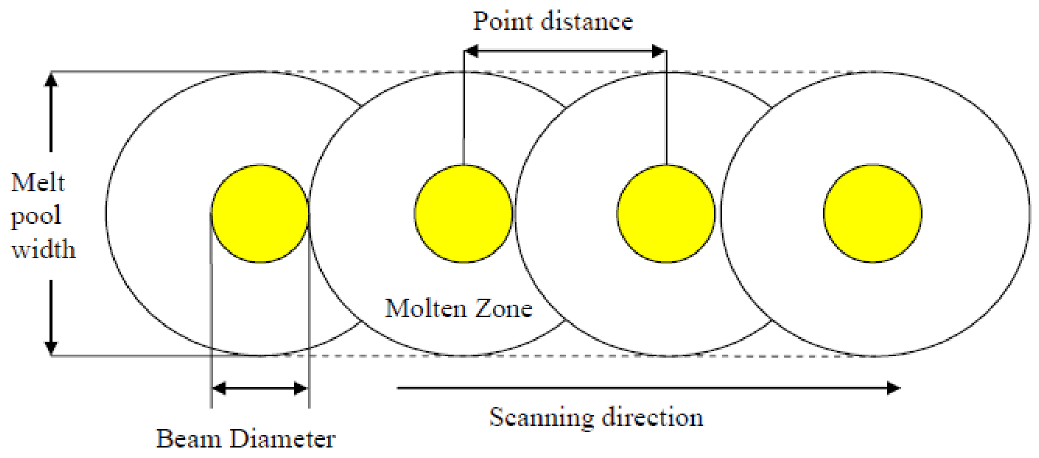

Fig. 2.16 Illustration of Point Distance Beam Diameter and Melt Pool Width.

The laser in SLM is not continuously scanned or fired across each scan line; it is fired in quick successive pulses, with quick pauses in between pulses, the interruption in between the pulses is in the microseconds (μs) range. This extremely quick interruption gives the illusion that the laser seems to be scanned continuously when observing the laser scans in a typical SLM build with the naked eye. Hence, as illustrated in Fig. 2.16, the point distance is the linear distance of the laser scanned during an exposure time as the laser is left to expose at each successive point. As the powder is melted along the laser scan lines, it creates a continuous molten zone known as the 'melt pool'. The melt pool solidifies when cooled, how fast a material solidify is dependent on the material's properties, in particular, its thermal conductivity. The melt pool can be further characterised by its melt pool width and length. Point distances and exposure times directly determine the scan velocity (v) of the laser; the relationship is shown by equation (2) [62],

$$\text{Scan Speed (V)} = \frac{\text{Point Distance}}{\text{Exposure Time}} \tag{2}$$

Dong found that increasing laser speed results in a non-linear decrease in the temperature of the powder bed surface [66]. Dewidar *et al*. observed the same effects of laser power and speed, and found that the density also increases as scan spacing decreases [67]. This finding effectively indicates that the density increases as the amount of energy delivered to the powder bed increases. Fig. 2.17 illustrates the definition of scan spacing. Scan spacing (h) is the distance between each successive scan line. The direction of the scan lines depicts how the laser scans the bed of powder on the substrate. The row of scan lines combine to forms a discrete pattern called 'Scan Strategy'. The scan strategy used in Fig. 2.17 is known as a 'Bi-directional' or 'Zig-Zag' scan strategy. Scan spacing (h) maybe pre-set to a value that allows the melt pool from a previous scan line to overlap with a previously solidified area.

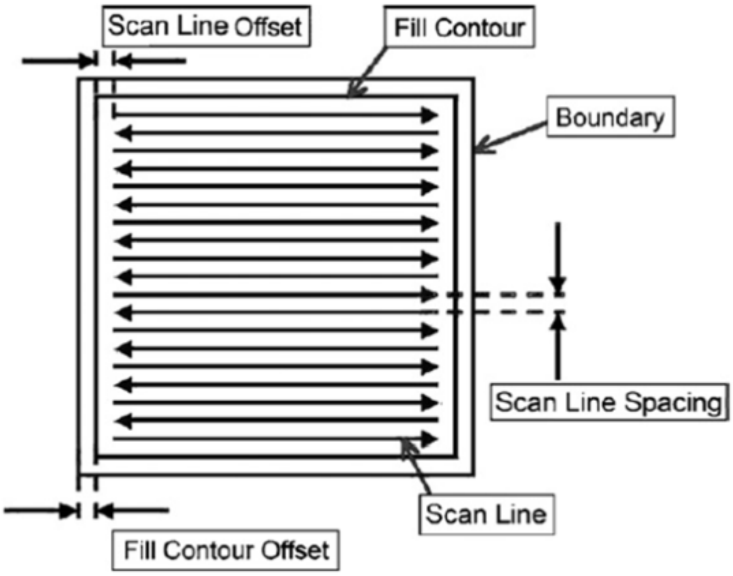

Fig. 2.17 Definition of Scan Spacing[68].

Layer thickness (t) is the pre-set distance the substrate or build platform is lowered after each build layer (Fig. 2.18), which is basically the thickness of the powder deposited for each layer. The layer thickness when the powder solidifies could vary from the originally pre-set layer thickness due to shrinkages during solidification. A removable Titanium substrate plate is used for performing the builds. The plate was pre-heated to 200 ℃ before the commencement of each build process, the purpose of the pre-heat is to reduce the residual stresses caused by rapid shrinkage and solidification from the laser melting. The results of excessive stresses would likely cause warping, bending or distortions to the component's final form which may affect its dimensional accuracy. The build is performed inside an inert gas chamber filled with argon. Although laser melting can commence when the argon inserting process reaches an argon gas pressure of 10 MBar and oxygen content of roughly 0.4%, as titanium is highly reactive with oxygen compared to other metals, especially at elevated temperatures.

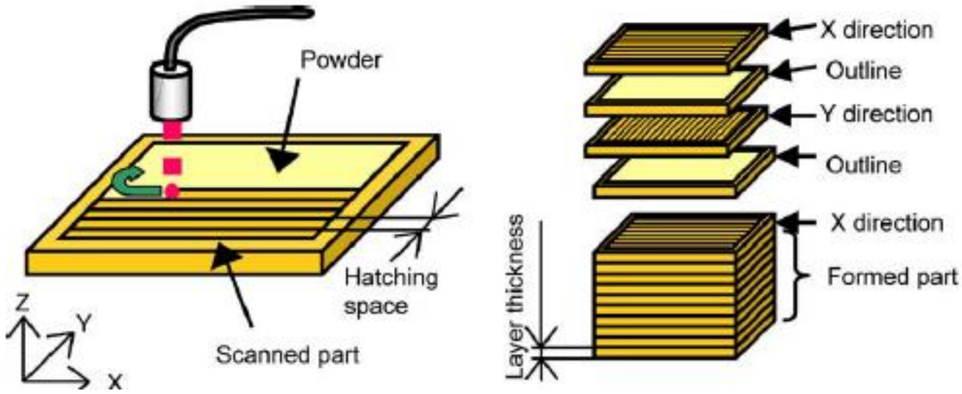

Fig. 2.18. Illustrating Layer Thickness [69].

2.4.3 Electron beam melting (EBM) fabrication method

In principle, electron beam melting (EBM) techniques have similar processing mechanism with the selective laser melting (SLM) techniques. Both can produce the nearly full density parts; differently, the EBM use an electron beam spot as the source to melt the powder [70, 71]. The building chamber is vacuumed before manufacturing the component. For electron beam melting systems, the range of the powder layer thickness is usually between 20 μm and 100 μm [72], which is also similar with the selective laser melting. Before manufacturing, the substrate plate need to be heated up to 700 ℃ by the electron beam to decrease residual stresses between the plate and the as-produced component, also this can help sinter powder together to avoid powder smoking [72, 73]. Numerous literatures have reported that experiments on the EBM as-produced specimens had been conducted to study their performance, and most of them were main focus on metals [73, 74, 75]. Meanwhile, plenty of biomedical applications including knee, hip joint and jaw replacements are being fabricated through EBM techniques [76, 77, 78].

2.4.3.1 Scanning parameters and patterns

Both EBM and SLM have similar working principle. A focused heat source selectively scans a powder bed. The scanned powder is melted and then rapidly solidifies. Once a layer is completed, the build platform descends by one layer thickness and a new layer of powder is deposited on top. The layer-by-layer process continues until the entire component has been completely produced. The main difference between the two processes origin of the heat source used, EBM is equipped with a tungsten filament to generate electron beam while SLM uses a laser. In addition, there are difference in the working conditions between the two techniques, including the chamber pressure and the pre-heating procedure. These can significantly alter the microstructure of the samples manufactured by the two technologies.

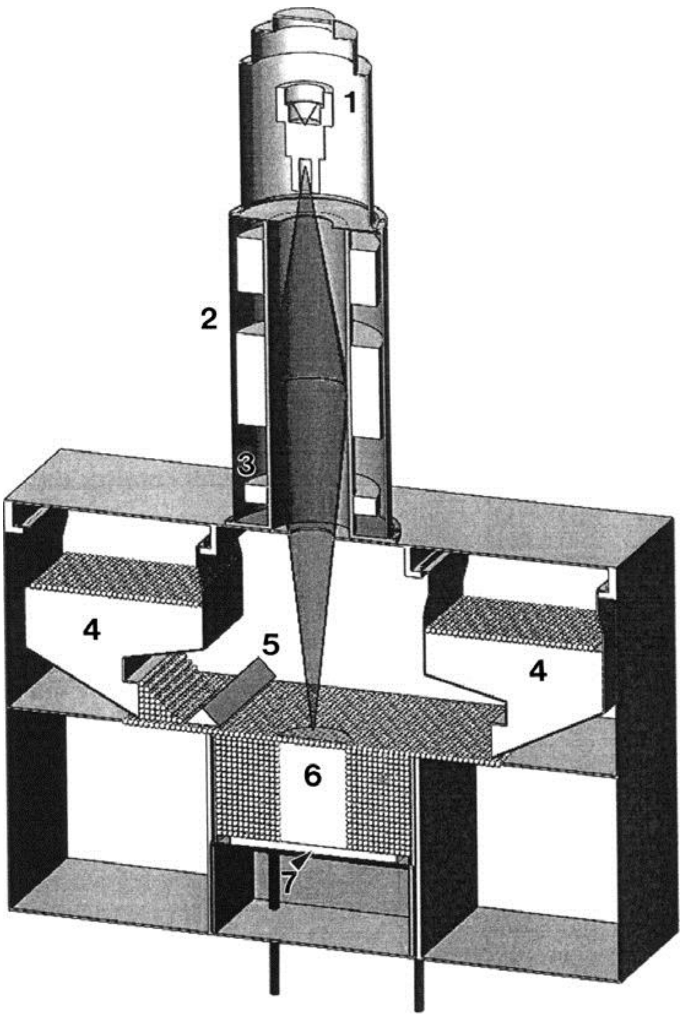

Fig. 2.19 The schematic rendering of EBM system [79].

The main structure and parts of the EBM are shown in Fig. 2.19 In the EBM system, the electron beam is generated in an electron gun (part 1) and focused on the powder bed controlled by the magnetic lenses (part 2). The metal powder is filled into the cassettes (part 4 in Fig. 2.19), the powder will be raked into the build table (part 5) and deposited on the substrate plate (part 6), which will be dropped during the building process. Prior to fabricating the component, the substrate plate is heated by the electron beam, the temperature is with a range of 500 ℃ to 730 ℃ depend on different metal powder. The electron beam spot is about 200 μm, which is larger than that of laser spot. The larger spot will create a bigger melting zone, consequently, the surface roughness is rougher than that of laser with smaller spot (Fig. 2.20).

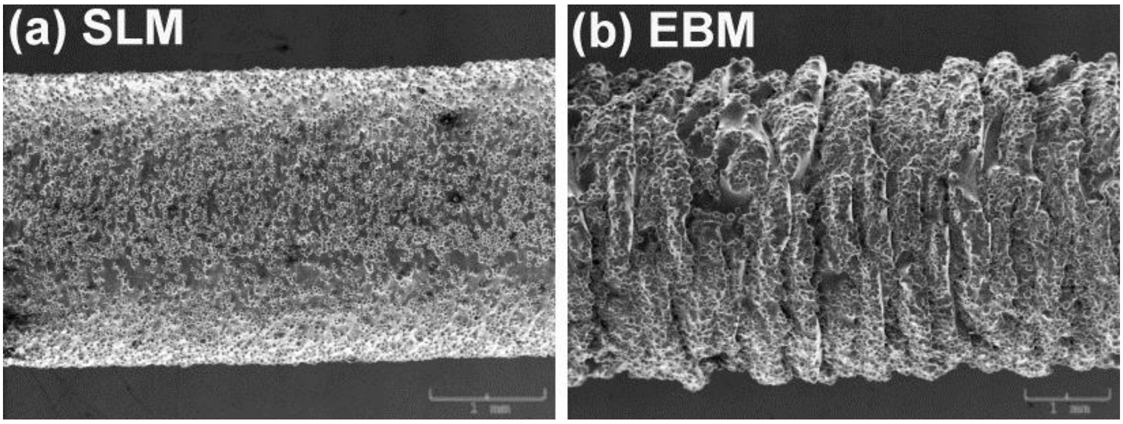

Fig. 2.20 The surface view of the SLM- and EBM-produced Ti-6Al-4V samples [80]

2.4.4 Powder material properties

For both SLM and EBM techniques, the material is the metal powder. The powder properties such as the particle size, the degree of spheroidization and the element composition, will affect the melting pool size, depth and shape, as well as melting the point and boiling point [62, 63, 65, 73], therefore, the quality of the powder not only determines the quality of the product, but also affects product stability.

A high-intensity laser beam selectively scans a thin powder bed, melting the metal particles, which solidify to form a solid layer. The build platform then moves down by the thickness of one layer (typically 50–100 μm), a new layer of powder is deposited on top and the process continues until the part is complete [81]. One of the key advantages of selective laser melting is its ability to produce near-full density metallic parts with a high degree of geometrical complexity. The particle size can determine the flow-ability and the layer density [82, 83]. The powder layer can be more compact with a condition of good flow-ability and suitable big-to-small ration powder particles [83]. The quality of the powder layer affect the final density of the AM-produced component, thus it is important to obtain more uniform and dense powder layer.

The powder temperature can reach evaporation during the melting process [15], as such the chemical composition of the metal powder is significant owing to its variation will change the melting point and boiling point, furthermore, the thermal conductivity will be affected by the powder nonuniformity, which was reported generating the defects such as the pores and thermal deformation [84, 85].

2.4.5 Unfavourable issues during SLM processing

It has been a challenge to obtain a full density component using AM techniques; however, there are many factors and parameters affecting the quality of the products. The AM process is affected by melting process, temperature gradients, solidification situation, surface tension and capillary [86], therefore unfavourable defects, including rough surface with powder adhesion, balling effect, defect pores, thermal deformation and balling effect could be generated in AM-produced components. As such it is necessary to deeply understand these defects formation mechanism and reduce them for further improvement of the quality of AM-produced products.

2.4.4.1 Powder adhesion

As the powder melting process is very complex, it is impossible to avoid the powder adhering on the strut surface for additive manufacturing techniques, and it might lead to negative accuracy of the open pore and strut for porous structure [87]. Furthermore, some powders adhered on the inside surface of the strut is very difficult to be removed and cleaned through post processing ways.

While the heat beam melting the powder bed, the input energy is absorbed by the selected scanned powder and then transferred to neighboured region, where the powders might get insufficient energy to be melted completely, consequently those powders are adhered on the edge of the solid part. Wang *et al*. found the same situation in their study on the influence of the SLM fabrication with single- and multiple-track [88] and made a similar conclusion. A heat affect zone (HAZ) will be formed during the melting process, and most of powders in this zone will be melted incompletely and evaluated to adhered powder on the surface (Fig. 2.21) [87].

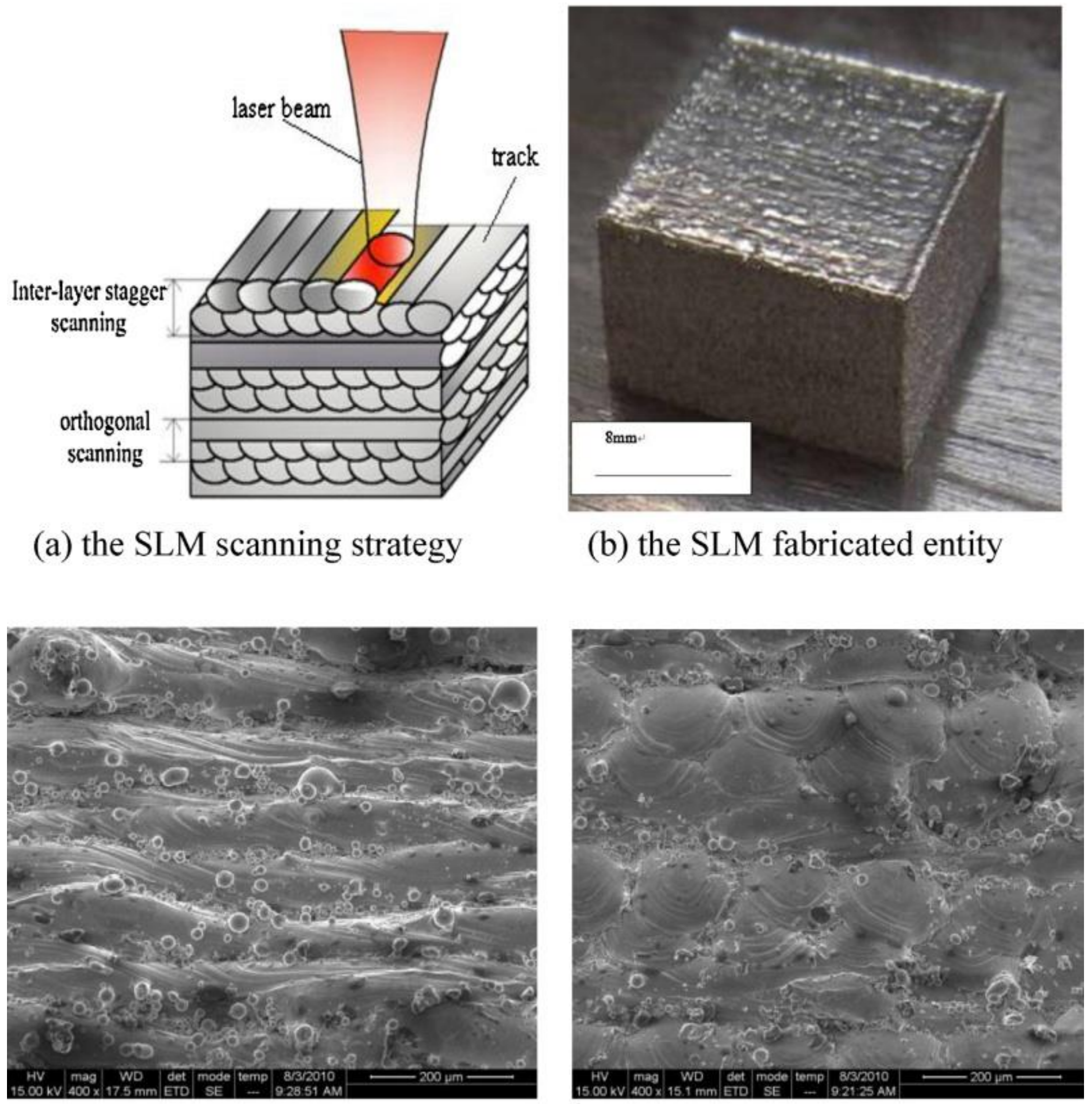

(a) the SLM scanning strategy (b) the SLM fabricated entity

(c) upper surface (d) side surface

Fig. 2.21 AM-produced component with rough surface [87]

2.4.4.2 Balling effect

The AM producing process is based on layer-wise method, in each layer, the powder is scanned with a strategy of line-by-line. The overlapping region is formed between any two of the scanning line, and its size is determined by the hatch space and the input energy. The optimized scanning parameters will create a continuous scanning track with cylindrical shape, otherwise, the track will be break if the input energy is insufficient, leading to reduction of overlapping region and generation of several metallic agglomerates of spherical shape, also named as balling effect [15, 65, 89]. As an undesirable phenomenon, balling effect can cause a weak interlayer. Balling effect can be eliminated under the condition of suitable parameters, with which the length-to-width ratio can be reduced.

2.4.4.3 Defect pores

The reasons of the defect pore generation are multiple and complex. Some defects are caused during the solidification of the keyhole in the centre of melt pool. The generation of a keyhole has an important effect on the melt pool depth during the SLM/EBM melting process [90, 91, 92]. A recoil pressure forms the metal vaporization and acts to push the liquid away from the melting zone, thereby forming a keyhole. The electron/laser beam can be reflected by the inner surface of the keyhole and the power is then concentrated at the bottom of keyhole. This causes a higher temperature at the bottom of the melting pool than the top. Thus, it is possible for the electron/laser beam to penetrate deeply into the material. If the cooling rate of the bottom is higher than that of top of the melt pool, a pore will be occurred. The defects generated during EBM/SLM process will affect the performance of the samples. The mechanism of defects formation during additive manufacturing process is complex and not yet fully understood [93]. Furthermore, duo to different melting and building process, the mechanism of some pore generation in SLM and EBM might be different. In SLM, some of the defect pores are evaluated from the gas bubbles (Fig. 2.22), which are formed during the fast melting and solidification process under the high chamber pressure [94]. In EBM, research on the defect pores in Ti-6Al-4V have indicated that, some pores come from the powder material and others might be generated from the metal evaporation [79, 80].

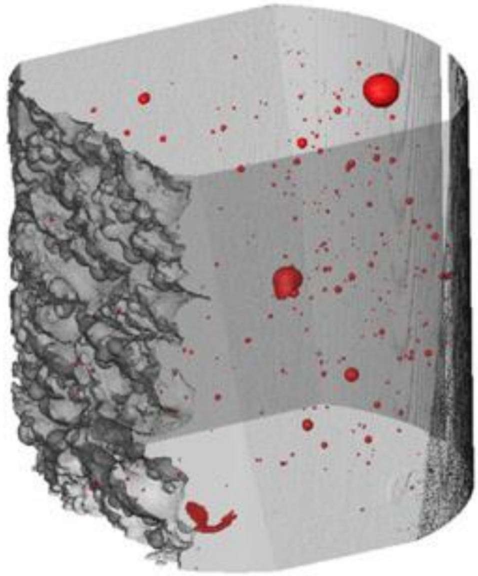

Fig. 2.22 Micro-CT image of the size and distribution of the defect pores [94].

For most metallic powders, the reported possible reasons for defects formation include powder defects [95], insufficient energy [96] , material vaporization [97] and imperfect collapse of the keyhole [98, 99]. Gong *et al*. [100] pointed out that the defects can have a negative influence on the tensile and fatigue properties of EBM/SLM-produced samples. Therefore, a detailed understanding is needed on mechanism of defect formation. During the EBM/SLM build process, the heat source has an approximate Gaussian distribution and is focused on the powder bed [101, 102].

2.4.4.3 Thermal deformation

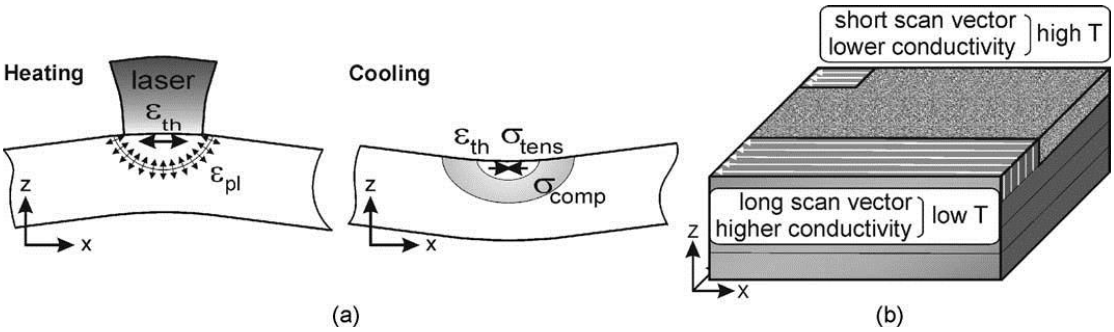

Fig. 2.23 The thermal deformation mechanism during the melting process [15]

The residual stresses are high in AM-produced parts as a result of a fast heating and cooling rate during melting process, they will lead to thermal deformation and thereby resulting in cracking and interlayer deboning. The specific reason of the formation of thermal deformation is the temperature gradient effect(Fig. 2.23), which is caused by the fast heating of the surface of the melt pool in the powder layer [15]. Expansion of the melt pool is transfer into elastic and plastic strains duo to limited expansion in neighbouring region. Once the metal material yield stress is reached, the centre of the melt pool will be compressed following with shrinkage after cooling down (Fig. 2.23). Thermal deformation can also be affected by the preheating as a result of a temperature gradient between the powder layer and substrate solid part [103].

2.4.4.4 Oxidations

It is generally believed that metallic materials, in particular titanium, are highly reactive with the surrounding oxygen atmosphere during the melting processing. This requires the use of a protective/vacuum atmosphere in the manufacturing process. Typically, the SLM/EBM process operates in a closed building compartment and the chamber is normally filled with argon or vacuum at a fixed pressure to avoid any oxidations. However, inaccurate adjustment of the gas pressure and a large amount of oxygen is adsorbed on the surface of the powder, so that the sample cannot be oxidized even under vacuum, thereby resulting in weak wettability. When the oxide is agitated into the bath, it can lead to entrainment of oxides causing the generation of pores and weak inter-mediate layers in the AM-produced parts [79].

2.4.5 AM microstructure

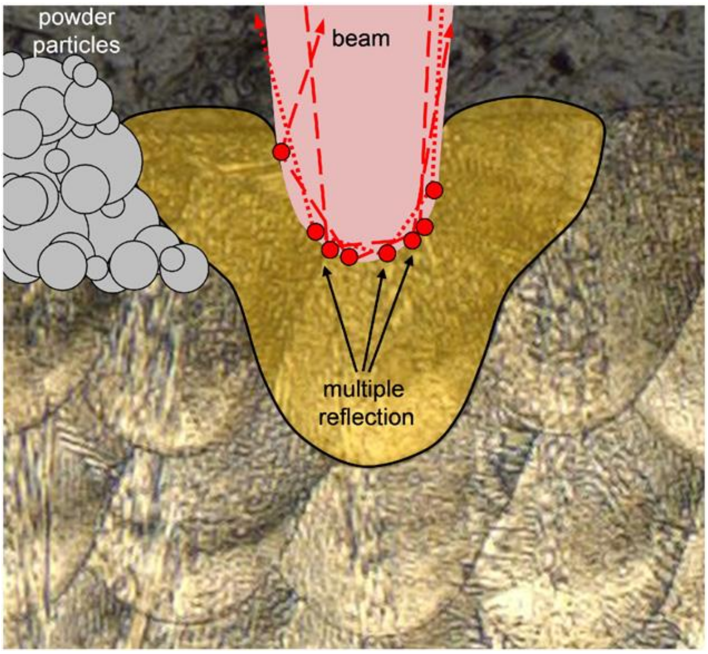

Fig. 2.24 The process of the SLM melting, within these keyholes, multiple reflections, absorption at the keyhole walls occur[104].

The AM-produced components exhibit different microstructure morphologies due to their different melting and solidification process. Fig 2.24 shows the process of the melting process, in which the melt pool can be seen clearly. The melting boundaries between the melting pools are considered as the Solid-liquid interface during the melting process [104]. As the input energy beam can only scan the surface of the powder bed, the underlying powder cannot absorb enough reflecting energy, this lead to the melt region smaller and the temperature lower than that of top powder bed, as such resulting in a key hole shape in melting pool.

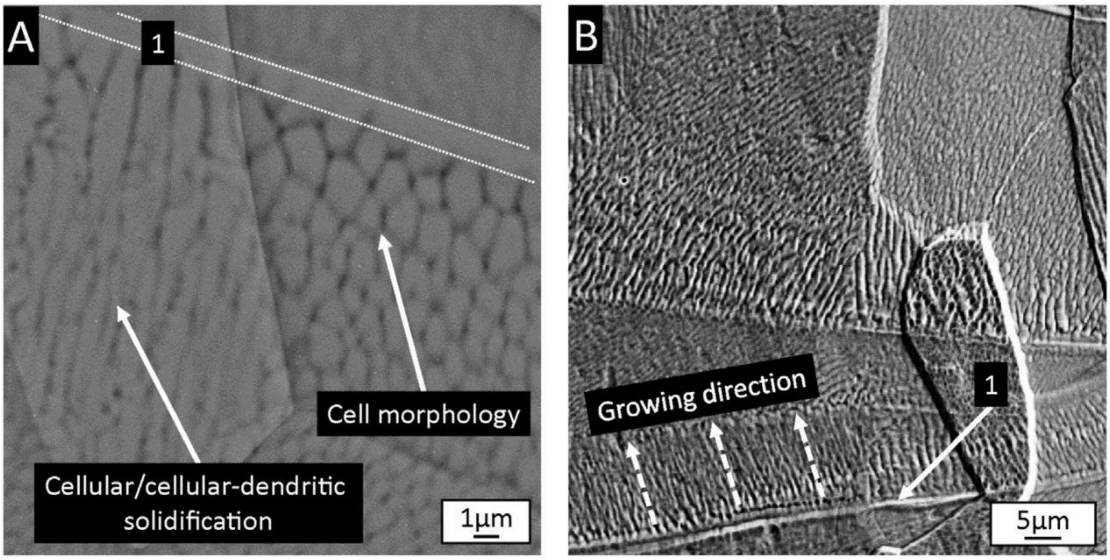

Fig. 2.25 The morphology of cellular/cellular-dendritic in the near-β titanium alloy Ti-5553[105].

The dendrite could be formed during the solidification process due to a gradient temperature distribution, which is caused by a different cooling rate between the melting pool centre and boundaries [105]. This results in a variation of the solidification morphology from boundary to the melt pool centre structures inside the melt pool (Fig. 2.25). The size of these cells varies from 1–3 μm, which is determined by the cooling rate. Fast-cooled melt, as occurring during melting for instance, often presents this type of solidification[105].

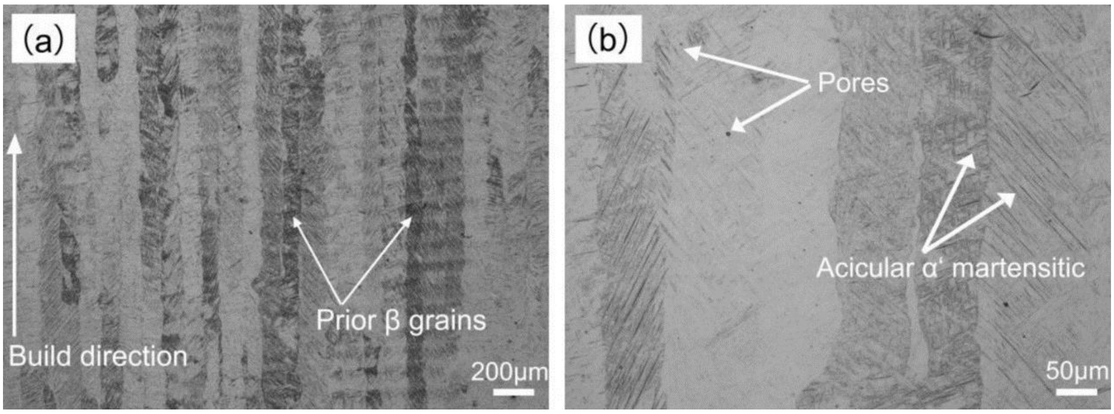

Fig. 2.26 SLM optical image of Ti-6Al-4V at the vertical direction[106]

Both SLM and EBM techniques have significant difference with conventional casting in solidification mechanism. It is reported that the cooling rate can reach at 10^4 K/s, therefore the microstructures have dramatic difference. The AM microstructures have a fine grain. Dai et al found that SLM microstructure contains big prior β grains and fine α' grains (Fig. 2.26) [106]. Zhao et al pointed out that α' phase can be formed in SLM process duo to a fast cooling rate [107]. Such an α' phase have not been found in EBM microstructure duo to its small cooling rate [107]. The EBM α lamellas size is coarser than that of SLM α' grain size (Figs. 2.27 and 2.28).

.

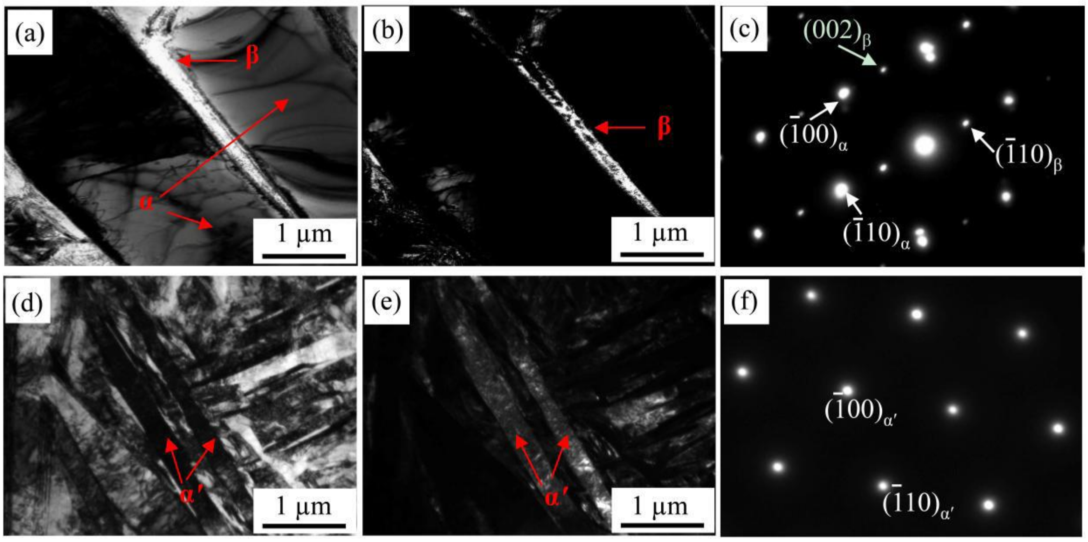

Fig. 2.27 The TEM image of the SLM and EBM for Ti-6Al4-V alloy [107]

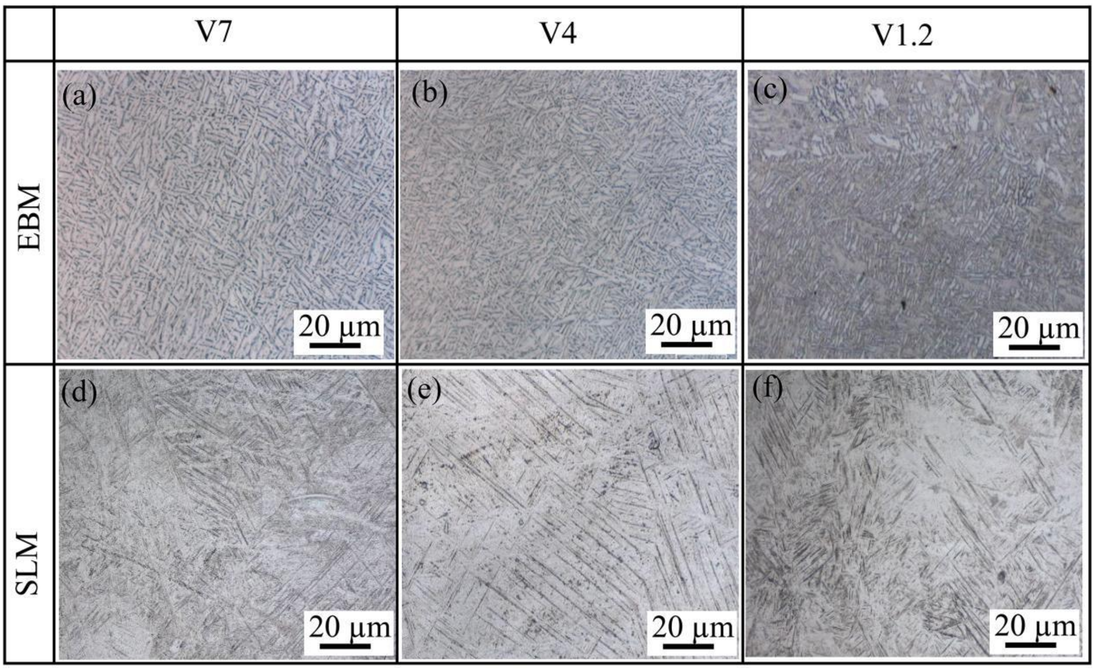

Fig. 2.28 The optical image of the SLM and EBM for Ti-6Al-4V [107]

2.4.6 AM mechanical properties

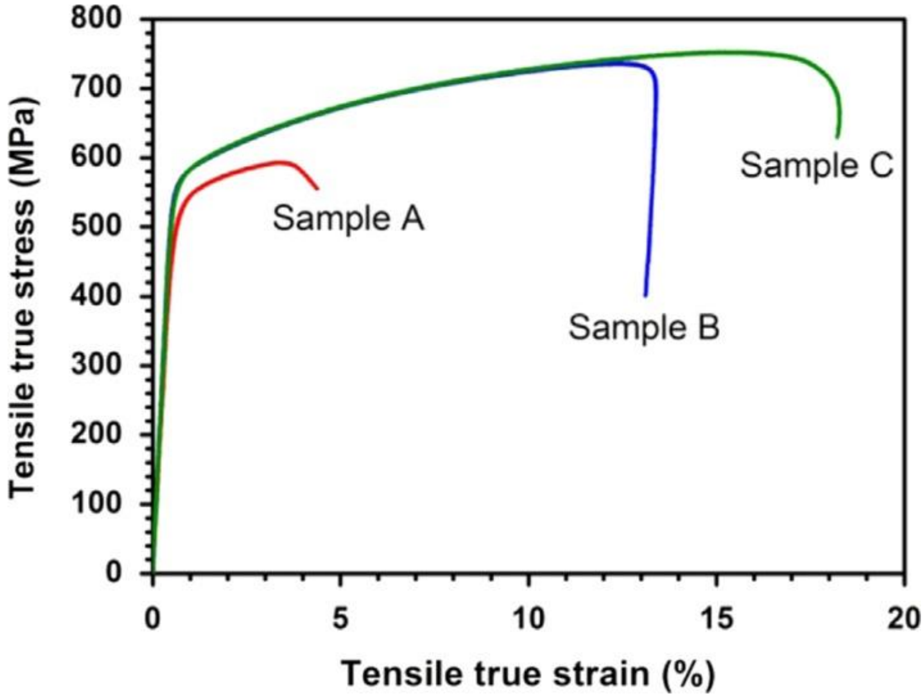

Fig. 2.29 The tensile stress-strain curves of the CP-titanium samples for SLM-produced(Sample A: P=85W, v=71mm/s, and relative density=96.4%; sample B: P=135W, v=112mm/s, and relative density=98.7%; and sample C: P=165W, V=138mm/s, and relative density=99.5%) [108].

It is well known that the mechanical properties of titanium alloy are significantly affected by the microstructure, consequently, the AM-produced components have different performance with the traditional casting parts in terms of the tensile and fatigue properties due to the unique microstructure or unfavourable defects [107, 108]. Attar *et al.* found that the tensile property of the CP-titanium can be affected by relative density, which is determined by the process parameters (Fig. 2.29) [108]. Rafi *et al.* compared the performance of the EBM- and SLM-produced specimens, based on microstructures and mechanical properties of Ti-6Al-4V specimens [109]. They found that the higher tensile strength obtained in SLM-produced Ti-6Al-4V owing to the martensitic microstructure, while the EBM-produced specimens contained a lamellar structure (Fig. 2.30).

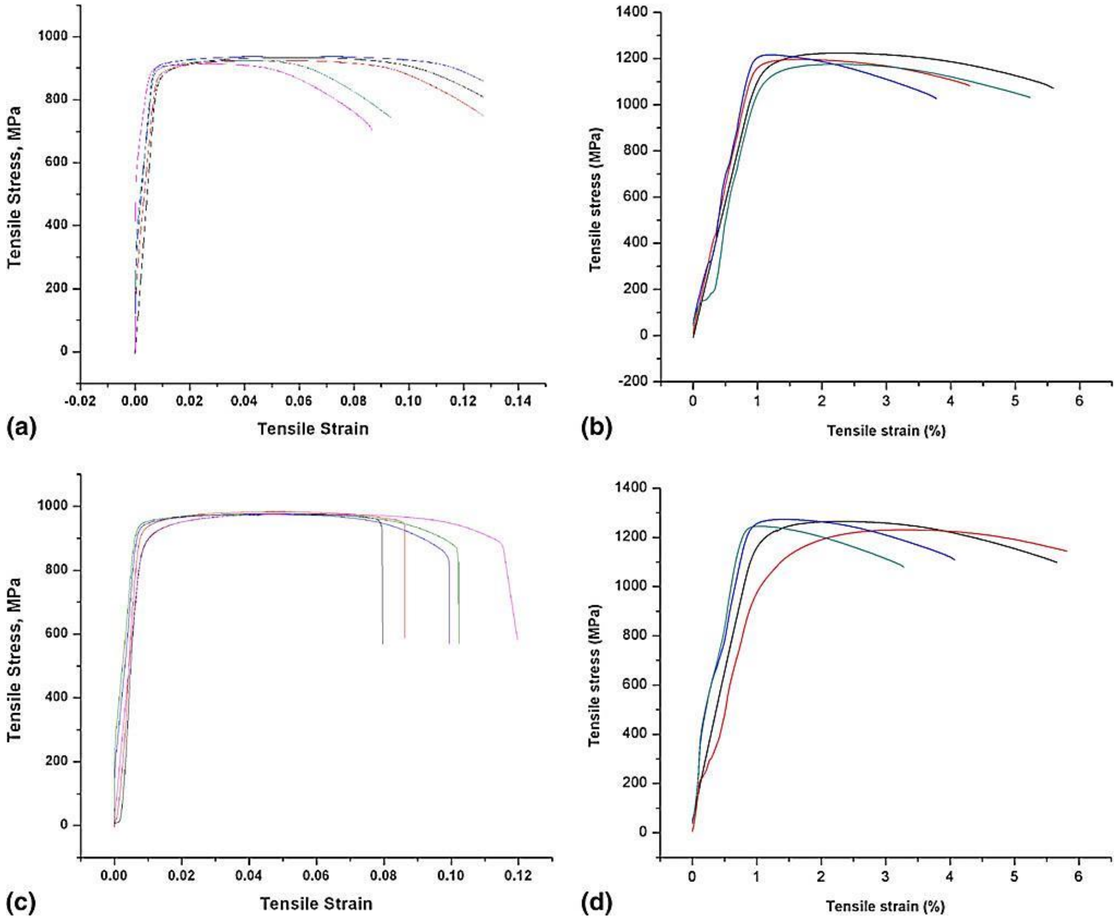

Fig. 2.30 Stress-Strain plots of Ti-6Al-4V specimens, (a) EBM specimen built in building direction, (b) SLM specimen built in building direction, (c) EBM specimen at x-y cross section and (d) SLM specimen built at x-y cross section[109].

Zhao *et al*. revealed that the small defects with the size less than 100 μm have limited effect on the tensile, but will affect the fatigue properties significantly [107]. The AM-produced samples have a comparable performance with the casting samples after hot isostatic pressing (HIP) treatment (Fig. 2.31).

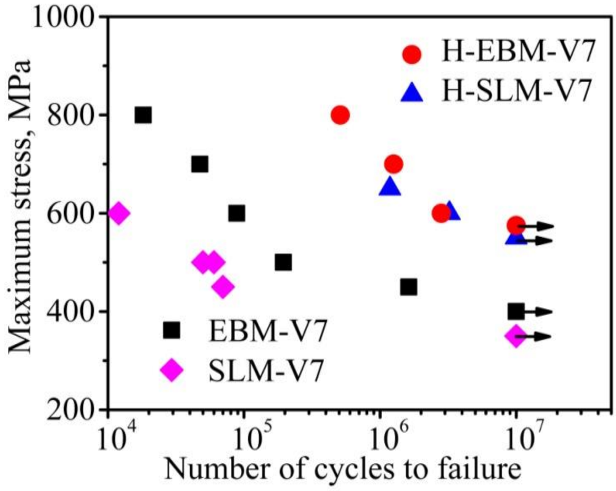

Fig. 2.31 S-N curves of AM-produced samples and HIP Ti–6Al–4V samples

2.4.7 AM corrosion properties

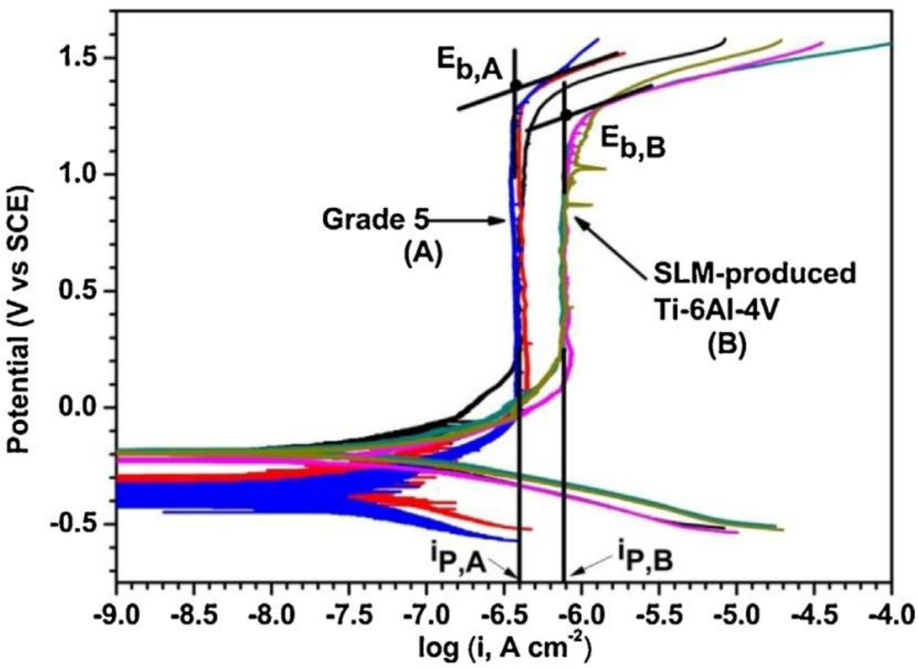

Fig. 2.32 The Potentiodynamic curves for the SLM-produced Ti-6Al-4 V alloy and commer-cial Grade 5 alloy in 3.5 wt.% NaCl solution [106].

It is well known that titanium alloys contain an excellent corrosion resistance ability as a result of generation of stable oxide film on the surface [1], and such a factor is very important for quality and life of implant. The layer-wised manufactured mechanism lead to distinguish microstructure for AM-produced components, which present similar or even better properties such as wear resistance. It is reported that the corrosion resistance of AM-produced Ti-6Al-4V could be improved due to laser gas nitriding. A nitride coating on the surface of component also can enhanced the corrosion resistance [110]. Hooyar *et al*. found that AM-produced CP-titanium alloy showed better wear property than that of conventional casting component [111]. However, Dai *et al.* pointed that the corrosion resistance of the SLM-produced Ti-6Al-4V components is weaker than conventional Grade 5 titanium alloy due to α' phase generation [106], which can be observed from the potentiodynamic curves (Fig. 2.32), the SLM-produced Ti-6Al-4V alloy sample exhibits a worse corrosion resistance than the commercial Grade 5 alloy over a broad range of potential. Furthermore, the AM-produced titanium alloys on different specimen planes present different microstructural characteristics thereby the corrosion resistance because of different scan strategies [110]. Dai *et al*. found that AM-produced sample x-y plane presented a better corrosion resistance compared to x-z cross section plane in 1 M HCl solution based on the electrochemical results (Fig. 2.33) [110].

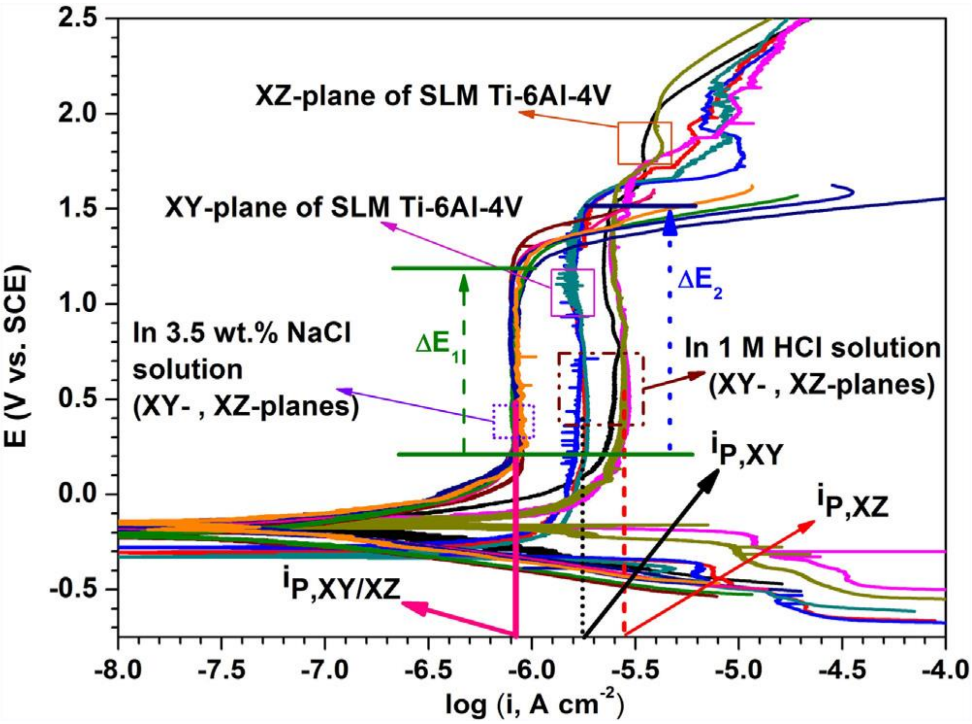

Fig. 2.33 The potentiodynamic curves for the x-y and x-z cross section plane of AM-produced specimens

2.5 Reference

[1] M. Geetha, A. Singh, R. Asokamani, A. Gogia, Ti based biomaterials, the ultimate choice for orthopaedic implants–A review, Progress in Materials Science. 54 (2009) 397-425.
[2] Bose S, Vahabzadeh S, Bandyopadhyay A. Bone tissue engineering using 3D printing, Materials Today. 16 (2013) 496-504.
[3] S. Kurtz, K. Ong, E. Lau, F. Mowat, M. Halpern, Projections of primary and revision hip and knee arthroplasty in the United States from 2005 to 2030, The Journal of Bone & Joint Surgery. 89 (2007) 780-785.
[4] M. Abdel-Hady Gepreel, M. Niinomi, Biocompatibility of Ti-alloys for long-term implantation, Journal of the Mechanical Behavior of Biomedical Materials. 20 (2013) 407-415
[5] G. Manivasagam, D. Dhinasekaran, A. Rajamanickam, Biomedical implants: corrosion and its prevention—a review, Recent Patents on Corrosion Science. 2 (2010) 40-54.
[6] R. LeGeros, S. Lin, R. Rohanizadeh, D. Mijares, J. LeGeros, Biphasic calcium phosphate bioceramics: preparation, properties and applications, Journal of Materials Science: Materials in Medicine. 14 (2003) 201-209.
[7] L. Zhang, D. Klemm, J. Eckert, Y. Hao, T. Sercombe, Manufacture by selective laser melting and mechanical behavior of a biomedical Ti–24Nb–4Zr–8Sn alloy, Scripta Materialia. 65 (2011) 21-24.
[8] Y. Hao, S. Li, S. Sun, C. Zheng, Q. Hu, R. Yang, Super-elastic titanium alloy with unstable plastic deformation, Applied Physics Letters. 87 (2005) 091906-091906-091903.
[9] J.A. Helsen, H. Jürgen Breme, Metals as biomaterials, Wiley, 1998.
[10] E.P. Lautenschlager, P. Monaghan, Titanium and titanium alloys as dental materials, International Dental Journal. 43 (1993) 245.
[11] R.R. Wang, A. Fenton, Titanium for prosthodontic applications: a review of the literature, Quintessence International. 27 (1996) 401.
[12] W. Wang, C.K. Poh, Titanium Alloys in Orthopaedics, 1 (2013) 1-20
[13] M. Taira, J. Moser, E. Greener, Studies of Ti alloys for dental castings, Dental Materials. 5 (1989) 45-50.
[14] K. Otsuka, C.M. Wayman, Shape memory materials, Cambridge University Press, 1999.
[15] J.-P. Kruth, L. Froyen, J. Van Vaerenbergh, P. Mercelis, M. Rombouts, B. Lauwers, Selective laser melting of iron-based powder, Journal of Materials Processing Technology. 149 (2004) 616-622.
[16] B.D. Ratner, A perspective on titanium biocompatibility, Springer, 2001.
[17] M. Andersson, B. Bergman, C. Bessing, G. Ericson, P. Lundquist, H. Nilson, Clinical results with titanium crowns fabricated with machine duplication and spark

erosion, Acta Odontologica. 47 (1989) 279-286.
[18] M.J. Donachie, Titanium: a technical guide, ASM international, 2000.
[19] M. Könönen, J. Kivilahti, Concise Review Biomaterials & Bioengineering: Fusing of Dental Ceramics to Titanium, Journal of Dental Research. 80 (2001) 848-854.
[20] C. R.G, Restorative dental material, 9th ed, St. Louis: Mosby, 1993.
[21] M.I. Froimson, J. Garino, A. Machenaud, J.P. Vidalain, Minimum 10-year results of a tapered, titanium, hydroxyapatite-coated hip stem: an independent review, The Journal of Arthroplasty. 22 (2007) 1-7.
[22] K.L. Wapner, Implications of metallic corrosion in total knee arthroplasty, Clinical Orthopaedics and Related Research. 271 (1991) 12-20.
[23] S. Nag, R. Banerjee, H.L. Fraser, Microstructural evolution and strengthening mechanisms in Ti–Nb–Zr–Ta, Ti–Mo–Zr–Fe and Ti–15Mo biocompatible alloys, Materials Science and Engineering: C. 25 (2005) 357-362.
[24] A. Gutiérrez, C. Munuera, M.F. López, J.A. Jiménez, C. Morant, T. Matzelle, N. Kruse, C. Ocal, Surface microstructure of the oxide protective layers grown on vanadium-free Ti alloys for use in biomedical applications, Surface Science. 600 (2006) 3780-3784.
[25] M. Niinomi, Mechanical properties of biomedical titanium alloys, Materials Science and Engineering: A. 243 (1998) 231-236.
[26] K. Zheng, X. Li, J. Fu, X. Fan, P. Wang, Y. Hao, S. Li, H. Fan, Z. Guo, Effects of Ti2448 half-pin with low elastic modulus on pin loosening in unilateral external fixation, Journal of Materials Science: Materials in Medicine. 22 (2011) 1579-1588.
[27] P. Janicki, G. Schmidmaier, What should be the characteristics of the ideal bone graft substitute? Combining scaffolds with growth factors and/or stem cells, Injury. 42 (2011) S77-S81.
[28] U. Kneser, D. Schaefer, B. Munder, C. Klemt, C. Andree, G. Stark, Tissue engineering of bone, Minimally Invasive Therapy & Allied Technologies. 11 (2002) 107-116.
[29] K. Alvarez, H. Nakajima, Metallic scaffolds for bone regeneration, Materials. 2 (2009) 790-832.
[30] H.-P. Degischer, B. Kriszt, Handbook Of Cellular Metals, Wiley-vch Weinheim, 2002.
[31] S.F. Hulbert, S.J. Morrison, J.J. Klawitter, Tissue reaction to three ceramics of porous and non-porous structures, Journal of Biomedical Materials Research. 6 (1972) 347-374.
[32] C.E. Holy, M.S. Shoichet, J.E. Davies, Engineering three-dimensional bone tissue in vitro using biodegradable scaffolds: Investigating initial cell-seeding density and culture period, Journal of Biomedical Materials Research. 51 (2000) 376-382.
[33] L. Yang, O. Harrysson, H. West, D. Cormier, Compressive properties of Ti–6Al–4V auxetic mesh structures made by electron beam melting, Acta Materialia. 60 (2012) 3370-3379.
[34] S. Yue, P.D. Lee, G. Poologasundarampillai, J.R. Jones, Evaluation of 3-D bioactive glass scaffolds dissolution in a perfusion flow system with X-ray microtomography, Acta Biomaterialia. 7 (2011) 2637-2643.

[35] C.M. Murphy, F.J. O'Brien, Understanding the effect of mean pore size on cell activity in collagen-glycosaminoglycan scaffolds, Cell Adhesion & Migration. 4 (2010) 377-381.
[36] J.E. Davies, Understanding peri-implant endosseous healing, Journal of Dental Education. 67 (2003) 932-949.
[37] T. Albrektsson, C. Johansson, Osteoinduction, osteoconduction and osseointegration, European Spine Journal. 10 (2001) S96-S101.
[38] W.G. DE LONG, T.A. Einhorn, K. Koval, M. McKee, W. Smith, R. Sanders, T. Watson, Bone grafts and bone graft substitutes in orthopaedic trauma surgery: a critical analysis, Journal of Bone and Joint Surgery. 89 (2007) 649-658.
[39] M. Geiger, R. Li, W. Friess, Collagen sponges for bone regeneration with rhBMP-2, Advanced Drug Delivery Reviews. 55 (2003) 1613-1629.
[40] U. Ripamonti, Osteoinduction in porous hydroxyapatite implanted in heterotopic sites of different animal models, Biomaterials. 17 (1996) 31-35.
[41] P. Griss, G. Heimke, Record of discussion on stability of joint prostheses, Biocompatibility Of Implant Materials. (1976) 52-68.
[42] S.J. Hollister, Porous scaffold design for tissue engineering, Nature Materials. 4 (2005) 518-524.
[43] A. Nouri, P.D. Hodgson, C.e. Wen, Biomimetic porous titanium scaffolds for orthopedic and dental applications, InTech, 2010.
[44] V. Karageorgiou, D. Kaplan, Porosity of 3D biomaterial scaffolds and osteogenesis, Biomaterials. 26 (2005) 5474-5491.
[45] A.C. Jones, C.H. Arns, D.W. Hutmacher, B.K. Milthorpe, A.P. Sheppard, M.A. Knackstedt, The correlation of pore morphology, interconnectivity and physical properties of 3D ceramic scaffolds with bone ingrowth, Biomaterials. 30 (2009) 1440-1451.
[46] F.G. Lyons, A.A. Al-Munajjed, S.M. Kieran, M.E. Toner, C.M. Murphy, G.P. Duffy, F.J. O'Brien, The healing of bony defects by cell-free collagen-based scaffolds compared to stem cell-seeded tissue engineered constructs, Biomaterials. 31 (2010) 9232-9243.
[47] P. Hui, P. Leung, A. Sher, Fluid conductance of cancellous bone graft as a predictor for graft-host interface healing, Journal of Biomechanics. 29 (1996) 123-132.
[48] S. Hollister, R. Maddox, J. Taboas, Optimal design and fabrication of scaffolds to mimic tissue properties and satisfy biological constraints, Biomaterials. 23 (2002) 4095-4103.
[49] S.J. Hollister, C. Lin, E. Saito, R. Schek, J. Taboas, J. Williams, B. Partee, C. Flanagan, A. Diggs, E. Wilke, Engineering craniofacial scaffolds, Orthodontics & Craniofacial Research. 8 (2005) 162-173.
[50] H.d.A. Almeida, P.J. da Silva Bártolo, Virtual topological optimisation of scaffolds for rapid prototyping, Medical Engineering & Physics. 32 (2010) 775-782.
[51] S. Sturm, S. Zhou, Y.-W. Mai, Q. Li, On stiffness of scaffolds for bone tissue engineering—a numerical study, Journal of Biomechanics. 43 (2010) 1738-1744.
[52] G.E. Ryan, A.S. Pandit, D.P. Apatsidis, Porous titanium scaffolds fabricated using a rapid prototyping and powder metallurgy technique, Biomaterials. 29 (2008)

3625-3635.
[53] G. Ryan, A. Pandit, D.P. Apatsidis, Fabrication methods of porous metals for use in orthopaedic applications, Biomaterials. 27 (2006) 2651-2670.
[54] D.A. Hollander, M. Von Walter, T. Wirtz, R. Sellei, B. Schmidt-Rohlfing, O. Paar, H.-J. Erli, Structural, mechanical and in vitro characterization of individually structured Ti–6Al–4V produced by direct laser forming, Biomaterials. 27 (2006) 955-963.
[55] N. Hopkinson, R. Hague, P. Dickens, Rapid manufacturing: an industrial revolution for the digital age, John Wiley & Sons, 2006.
[56] G.N. Levy, R. Schindel, J.P. Kruth, Rapid manufacturing and rapid tooling with layer manufacturing (lm) technologies, state of the art and future perspectives, CIRP Annals - Manufacturing Technology. 52 (2003) 589-609.
[57] J.-P. Kruth, M. Leu, T. Nakagawa, Progress in additive manufacturing and rapid prototyping, CIRP Annals-Manufacturing Technology. 47 (1998) 525-540.
[58] H. Schleifenbaum, W. Meiners, K. Wissenbach, C. Hinke, Individualized production by means of high power Selective Laser Melting, CIRP Journal of Manufacturing Science and Technology. 2 (2010) 161-169.
[59] E. Yasa, J. Deckers, J.-P. Kruth, The investigation of the influence of laser re-melting on density, surface quality and microstructure of selective laser melting parts, Rapid Prototyping Journal. 17 (2011) 312-327.
[60] E. Olakanmi, R. Cochrane, K. Dalgarno, Densification mechanism and microstructural evolution in selective laser sintering of Al–12Si powders, Journal of Materials Processing Technology. 211 (2011) 113-121.
[61] R. Li, J. Liu, Y. Shi, L. Wang, W. Jiang, Balling behavior of stainless steel and nickel powder during selective laser melting process, The International Journal of Advanced Manufacturing Technology. 59 (2012) 1025-1035.
[62] A. Simchi, Direct laser sintering of metal powders: mechanism, kinetics and microstructural features, Materials Science and Engineering: A. 428 (2006) 148-158.
[63] E. Brandl, U. Heckenberger, V. Holzinger, D. Buchbinder, Additive manufactured AlSi10Mg samples using Selective Laser Melting (SLM): Microstructure, high cycle fatigue, and fracture behavior, Materials & Design. 34 (2012) 159-169.
[64] S. Dadbakhsh, L. Hao, P. Jerrard, D. Zhang, Experimental investigation on selective laser melting behaviour and processing windows of in situ reacted Al/Fe_2O_3 powder mixture, Powder Technology. 231 (2012) 112-121.
[65] J.-P. Kruth, P. Mercelis, J. Van Vaerenbergh, L. Froyen, M. Rombouts, Binding mechanisms in selective laser sintering and selective laser melting, Rapid Prototyping Journal. 11 (2005) 26-36.
[66] H.-D. Deng, J. Liu, W.-R. Zhao, W. Zhang, X.-S. Lin, T. Sun, Q.-F. Dai, L.-J. Wu, S. Lan, A.V. Gopal, Enhancement of switching speed by laser-induced clustering of nanoparticles in magnetic fluids, Applied Physics Letters. 92 (2008) 233103.
[67] M.M. Dewidar, K.W. Dalgarno, C.S. Wright, Processing conditions and mechanical properties of high-speed steel parts fabricated using direct selective laser sintering, Proceedings of the Institution of Mechanical Engineers, Part B: Journal of Engineering Manufacture. 217 (2003) 1651-1663.
[68] L. Hao, S. Dadbakhsh, O. Seaman, M. Felstead, Selective laser melting of a

stainless steel and hydroxyapatite composite for load-bearing implant development, Journal of Materials Processing Technology. 209 (2009) 5793-5801.
[69] K. Osakada, M. Shiomi, Flexible manufacturing of metallic products by selective laser melting of powder, International Journal of Machine Tools and Manufacture. 46 (2006) 1188-1193.
[70] L.E. Murr, S.M. Gaytan, D.A. Ramirez, E. Martinez, J. Hernandez, K.N. Amato, P.W. Shindo, F.R. Medina, R.B. Wicker, Metal fabrication by additive manufacturing using laser and electron beam melting technologies, Journal of Materials Science & Technology. 28 (2012) 1-14.
[71] N. Hrabe, T. Quinn, Effects of processing on microstructure and mechanical properties of a titanium alloy (Ti–6Al–4V) fabricated using electron beam melting (EBM), Part 2: Energy input, orientation, and location, Materials Science and Engineering: A. 573 (2013) 271-277.
[72] S.L. Sing, J. An, W.Y. Yeong, F.E. Wiria, Laser and electron‐beam powder‐bed additive manufacturing of metallic implants: A review on processes, materials and designs, Journal of Orthopaedic Research. 34 (2015) 369-385.
[73] S. Li, L. Murr, X. Cheng, Z. Zhang, Y. Hao, R. Yang, F. Medina, R. Wicker, Compression fatigue behavior of Ti–6Al–4V mesh arrays fabricated by electron beam melting, Acta Materialia. 60 (2012) 793-802.
[74] S. Li, Q. Xu, Z. Wang, W. Hou, Y. Hao, R. Yang, L. Murr, Influence of cell shape on mechanical properties of Ti–6Al–4V meshes fabricated by electron beam melting method, Acta Biomaterialia. 10 (2014) 4537-4547.
[75] S. Zhao, S. Li, W. Hou, Y. Hao, R. Yang, R. Misra, The influence of cell morphology on the compressive fatigue behavior of Ti-6Al-4V meshes fabricated by electron beam melting, Journal of the Mechanical Behavior of Biomedical Materials. 59 (2016) 251-264.
[76] M. Cronskär, M. Bäckström, L.-E. Rännar, Production of customized hip stem prostheses-a comparison between conventional machining and electron beam melting (EBM), Rapid Prototyping Journal. 19 (2013) 365-372.
[77] A. Mazzoli, M. Germani, R. Raffaeli, Direct fabrication through electron beam melting technology of custom cranial implants designed in a PHANToM-based haptic environment, Materials & Design. 30 (2009) 3186-3192.
[78] A.L. Jardini, M.A. Larosa, R. Maciel Filho, C.A. de Carvalho Zavaglia, L.F. Bernardes, C.S. Lambert, D.R. Calderoni, P. Kharmandayan, Cranial reconstruction: 3D biomodel and custom-built implant created using additive manufacturing, Journal of Cranio-Maxillofacial Surgery. 42 (2014) 1877-1884.
[79] D. Ramirez, L. Murr, E. Martinez, D. Hernandez, J. Martinez, B. Machado, F. Medina, P. Frigola, R. Wicker, Novel precipitate–microstructural architecture developed in the fabrication of solid copper components by additive manufacturing using electron beam melting, Acta Materialia. 59 (2011) 4088-4099.
[80] M. Koike, P. Greer, K. Owen, G. Lilly, L.E. Murr, S.M. Gaytan, E. Martinez, T. Okabe, Evaluation of titanium alloys fabricated using rapid prototyping technologies—electron beam melting and laser beam melting, Materials. 4 (2011) 1776-1792.

[81] L. Thijs, F. Verhaeghe, T. Craeghs, J.V. Humbeeck, J.-P. Kruth, A study of the microstructural evolution during selective laser melting of Ti–6Al–4V, Acta Materialia. 58 (2010) 3303-3312.
[82] I. Yadroitsev, A. Gusarov, I. Yadroitsava, I. Smurov, Single track formation in selective laser melting of metal powders, Journal of Materials Processing Technology. 210 (2010) 1624-1631.
[83] M.A. Meyers, E.A. Olevsky, Sintering Theory and Practice, Journal of Materials Engineering and Performance. 6 (1997) 278.
[84] A. Hussein, L. Hao, C. Yan, R. Everson, Finite element simulation of the temperature and stress fields in single layers built without-support in selective laser melting, Materials & Design. 52 (2013) 638-647.
[85] E. Sallica-Leva, A. Jardini, J. Fogagnolo, Microstructure and mechanical behavior of porous Ti–6Al–4V parts obtained by selective laser melting, Journal of the mechanical behavior of biomedical materials. 26 (2013) 98-108.
[86] X. Zhou, D. Wang, X. Liu, D. Zhang, S. Qu, J. Ma, G. London, Z. Shen, W. Liu, 3D-imaging of selective laser melting defects in a Co–Cr–Mo alloy by synchrotron radiation micro-CT, Acta Materialia. 98 (2015) 1-16.
[87] D. Wang, Y. Yang, R. Liu, D. Xiao, J. Sun, Study on the designing rules and processability of porous structure based on selective laser melting (SLM), Journal of Materials Processing Technology. 213 (2013) 1734-1742.
[88] W. Di, Y. Yongqiang, S. Xubin, C. Yonghua, Study on energy input and its influences on single-track, multi-track, and multi-layer in SLM, The International Journal of Advanced Manufacturing Technology. 58 (2012) 1189-1199.
[89] X. Liu, P.K. Chu, C. Ding, Surface modification of titanium, titanium alloys, and related materials for biomedical applications, Materials Science and Engineering: R: Reports. 47 (2004) 49-121.
[90] J.H. Cho, S.J. Na, J.H. Cho, S.J. Na, Implementation of real-time multiple reflection and Fresnel absorption of laser beam in keyhole, Journal of Physics D: Applied Physics. 39 (2006) 5372-5378.
[91] S.A. Tsirkas, P. Papanikos, T. Kermanidis, Numerical simulation of the laser welding process in butt-joint specimens, Journal of Materials Processing Technology. 134 (2003) 59-69.
[92] R. Rai, P. Burgardt, J.O. Milewski, T.J. Lienert, T. Debroy, Heat transfer and fluid flow during electron beam welding of 21Cr–6Ni–9Mn steel and Ti–6Al–4V alloy, Journal of Physics D: Applied Physics. 42 (2009) 25503-25514.
[93] X. Tan, Y. Kok, Y.J. Tan, M. Descoins, D. Mangelinck, S.B. Tor, K.F. Leong, C.K. Chua, Graded microstructure and mechanical properties of additive manufactured Ti–6Al–4V via electron beam melting, Acta Materialia. 97 (2015) 1-16.
[94] S. Tammas-Williams, H. Zhao, F. Léonard, F. Derguti, I. Todd, P. Prangnell, XCT analysis of the influence of melt strategies on defect population in Ti–6Al–4V components manufactured by selective electron beam melting, Materials Characterization. 102 (2015) 47-61.
[95] S.M. Gaytan, L.E. Murr, F. Medina, E. Martinez, M.I. Lopez, R.B. Wicker, Advanced metal powder based manufacturing of complex components by electron

beam melting, Materials Technologys. 24 (2009) 180-190.
[96] L.C. Zhang, T.B. Sercombe, Selective Laser Melting of Low-Modulus Biomedical Ti-24Nb-4Zr-8Sn Alloy: Effect of Laser Point Distance, Key Engineering Materials. 520 (2012) 226-233.
[97] D. Dai, D. Gu, Effect of metal vaporization behavior on keyhole-mode surface morphology of selective laser melted composites using different protective atmospheres, Apply Surfce Science. 355 (2015) 310–319.
[98] H. Zhao, T. Debroy, Pore formation during laser beam welding of die-cast magnesium alloy AM60B - mechanism and remedy, Weld Journal. 80 (2001) 204-210.
[99] M. Courtois, M. Carin, P.L. Masson, S. Gaied, M. Balabane, A new approach to compute multi-reflections of laser beam in a keyhole for heat transfer and fluid flow modelling in laser welding, Journal of Physics D: Applied Physics. 46 (2013) 505305.
[100] H. Gong, K. Rafi, H. Gu, G.D.J. Ram, T. Starr, B. Stucker, Influence of defects on mechanical properties of Ti–6Al–4V components produced by selective laser melting and electron beam melting, Materials & Design. 86 (2015) 545–554.
[101] P. Lemasson, M. Carin, J.C. Parpillon, R. Berthet, 2D-heat transfer modelling within limited regions using moving sources: application to electron beam welding, International Journal of Heat and Mass Transfer. 46 (2003) 4553–4559.
[102] J.M. Dowden, The mathematics of thermal modeling: an introduction to the theory of laser material processing, CRC Press, Boca Raton, 2001.
[103] H. Yves-Christian, W. Jan, M. Wilhelm, W. Konrad, P. Reinhart, Net shaped high performance oxide ceramic parts by selective laser melting, Physics Procedia. 5 (2010) 587-594.
[104] M. Cloots, P.J. Uggowitzer, K. Wegener, Investigations on the microstructure and crack formation of IN738LC samples processed by selective laser melting using Gaussian and doughnut profiles, Materials & Design. 89 (2016) 770-784.
[105] H. Schwab, F. Palm, U. Kühn, J. Eckert, Microstructure and mechanical properties of the near-beta titanium alloy Ti-5553 processed by selective laser melting, Materials & Design. 105 (2016) 75-80.
[106] N. Dai, L.-C. Zhang, J. Zhang, Q. Chen, M. Wu, Corrosion behavior of selective laser melted Ti-6Al-4V alloy in NaCl solution, Corrosion Science. 102 (2016) 484-489.
[107] X. Zhao, S. Li, M. Zhang, Y. Liu, T.B. Sercombe, S. Wang, Y. Hao, R. Yang, L.E. Murr, Comparison of the microstructures and mechanical properties of Ti–6Al–4V fabricated by selective laser melting and electron beam melting, Materials & Design. 95 (2016) 21-31.
[108] H. Attar, M. Calin, L. Zhang, S. Scudino, J. Eckert, Manufacture by selective laser melting and mechanical behavior of commercially pure titanium, Materials Science and Engineering: A. 593 (2014) 170-177.
[109] H. Rafi, N. Karthik, H. Gong, T.L. Starr, B.E. Stucker, Microstructures and mechanical properties of Ti6Al4V parts fabricated by selective laser melting and electron beam melting, Journal of materials engineering and performance. 22 (2013) 3872-3883.
[110] N. Dai, L.-C. Zhang, J. Zhang, X. Zhang, Q. Ni, Y. Chen, M. Wu, C. Yang, Distinction in Corrosion Resistance of Selective Laser Melted Ti-6Al-4V Alloy on

Different Planes, Corrosion Science. 111 (2016) 703-710.
[111] H. Attar, M. Bönisch, M. Calin, L.C. Zhang, K. Zhuravleva, A. Funk, S. Scudino, C. Yang, J. Eckert, Comparative study of microstructures and mechanical properties of in situ Ti-TiB composites produced by selective laser melting, powder metallurgy, and casting technologies, Journal of Materials Research. 29 (2014) 1941-1950.

Chapters 3, 4, 5, and 6 are not included in this version of the thesis due to Copyright reasons. The chapters have been published in the following articles:

Chapter 3:

Liu, Y. J., Li, X. P., Zhang, L. C., & Sercombe, T. B. (2015). Processing and properties of topologically optimised biomedical Ti–24Nb–4Zr–8Sn scaffolds manufactured by selective laser melting. *Materials Science and Engineering: A*, *642*, 268-278. doi:10.1016/j.msea.2015.06.088.

Chapter 4:

Liu, Y.J., Li, S.J., Hou, W.T., Wang, S.G., Hao, Y.L., Yang, R., Sercombe, T., & Zhang, L.C. (2016). Electron beam melted beta-type Ti-24Nb-4Zr-8Snporous structures with high strength-to-modulus ratio, *Journal of Materials Science and Technology, 32*, 505-508. doi:10.1016/j.jmst.2016.03.020

Chapter 5:

Liu, Y. J., Li, S. J., Wang, H. L., Hou, W. T., Hao, Y. L., Yang, R., ... & Zhang, L. C. (2016). Microstructure, defects and mechanical behavior of beta-type titanium porous structures manufactured by electron beam melting and selective laser melting. *Acta Materialia*, *113*, 56-67. doi:10.1016/j.actamat.2016.04.029

Chapter 6:

Liu, Y. J., Wang, H. L., Li, S. J., Wang, S. G., Wang, W. J., Hou, W. T., ... & Zhang, L. C. (2017). Compressive and fatigue behavior of beta-type titanium porous structures fabricated by electron beam melting. *Acta Materialia*, *126*, 58-66. doi:10.1016/j.actamat.2016.12.052.

7. Summary

Additive manufacturing is gaining increasing attention in medicine fields, especially in dental and implant areas. Because the AM-produced components perform various advantages in comparison to counterparts made by traditional technologies, such as ability to manufacture scaffold structure for complex component, high material utilization, support of tissue growth and the unique customized service for individual patient, additive manufacturing is considered to have a large potential market. AM-produced implant have been considered as the most promising alternative technologies to help make pre-operative planning for patient-specific, reduce the surgery operation time and improve the success rate of implant surgery. Base on the biomedical titanium materials, the 3D printing technologies have great potential in the precision medicine and community health. The research presented in this PhD thesis was focused on the manufacturing of Ti-based materials using AM techniques, which include SLM and EBM, being potential for biomedical applications. To this end, AM manufacturing parameters was investigated and optimized in order to fabricate porous beta-type titanium alloy parts. Afterwards, characterizations, microstructures and mechanical properties of the processed components were studied in order to further understand the relationships between microstructure and mechanical properties as follow:

First of all, the high relative density porous specimens were produced by both SLM and EBM techniques. The shape and amount of pores inside the solid strut of scaffold were mapped using Micro CT, which clearly showed the difference of distribution of pores with different laser scan speeds. The evaporation of tin during SLM process it thought to be a major contributor to the increase in porosity that occurs at the slower scan speeds. The scan speed also had an influence on the size of the struts produced, however the effect was significant only in the building (Z) direction.

Moreover, the reason of defect generations were studied. The laser beam spot size of ~40 μm is much smaller than the electron beam spot of ~200μm which leads to differences in width and depth of the melt pool. The width of melt pool in the EBM sample is larger than that in SLM. This is a result of the higher pre-heating temperature and energy density input in EBM process. The smaller spot size of the SLM process results in a deeper keyhole caused by radiation reflection, thereby leading to a deeper melt pool in SLM than that in EBM.

Furthermore, the relationship of the microstructures, defects and the compressive properties were discussed. The fine single β phase dendrites in the as-fabricated SLM samples results in high compressive strength (~50 ±0.9 MPa). During annealing of the SLM samples at 750 °C, the β grains coarsen and the fine dendrites dissolve. This decreases the strength of the SLM samples by nearly 20%. For the EBM samples, annealing dissolves α phase, which, along with grain growth, decreases the strength. Small defects have limited influence on compressive properties for both EBM and SLM samples.

In addition, the relationship of the microstructures and the fatigue properties were studied. The unique manufacturing process of the EBM results in formation of different sizes of grains. Therefore, the apparent fatigue crack deflection occurs in the columnar grain zone duo to large misorientation between the adjacent grains. Compared with Ti-6Al-4V samples, the Ti2448 porous samples exhibit a higher normalized fatigue strength owing to the super-elastic property and the larger plastic zone ahead of the fatigue crack tip. For the same fatigue strength, the Young's modulus of Ti2448 porous samples is only half of Ti-6Al-4V porous samples.